N-Phenyl-4-pyrazolo[1,5-*b*]pyridazin-3-ylpyrimidin-2-amines as Potent and Selective Inhibitors of Glycogen Synthase Kinase 3 with Good Cellular Efficacy

Francis X. Tavares,*[†] Joyce A. Boucheron,[‡] Scott H. Dickerson,[§] Robert J. Griffin,[||] Frank Preugschat,[⊥] Stephen A. Thomson,[†] Tony Y. Wang,[‡] and Hui-Qiang Zhou[†]

Department of Medicinal Chemistry, Department of Metabolic Diseases, Department of Computational, Analytical and Structural Sciences, Department of Research Bioanalysis and Drug Metabolism, and Department of Biochemical and Analytical Pharmacology, GlaxoSmithKline, Research Triangle Park, North Carolina 27709

Received March 11, 2004

Glycogen synthase kinase 3 regulates glycogen synthase, the rate-determining enzyme for glycogen synthesis. Liver and muscle glycogen synthesis is defective in type 2 diabetics, resulting in elevated plasma glucose levels. Inhibition of GSK-3 could potentially be an effective method to control plasma glucose levels in type 2 diabetics. Structure−activity studies on a *N*-phenyl-4-pyrazolo[1,5-*b*]pyridazin-3-ylpyrimidin-2-amine series have led to the identification of potent and selective compounds with good cellular efficacy. Molecular modeling studies have given insights into the mode of binding of these inhibitors. Since the initial leads were also potent inhibitors of CDK-2/CDK-4, an extensive SAR was performed at various positions of the pyrazolo[1,5-*b*]pyridazin core to afford potent GSK-3 inhibitors that were highly selective over CDK-2. In addition, these inhibitors also exhibited very good cell efficacy and functional response. A representative example was shown to have good oral exposure levels, extending their utility in an in vivo setting. These inhibitors provide a viable lead series in the discovery of new therapies for the treatment of type 2 diabetes.

Introduction

Glycogen synthase kinase 3 (GSK-3) is a ubiquitously expressed serine/threonine protein kinase, originally identified as an enzyme that regulates glycogen synthase (GS) in response to insulin.[1] There are two highly homologous forms of mammalian GSK-3, designated α and *β*, with molecular weights of 51 and 46 kDa, respectively, and catalytic domains with about 90% identity.[2] The differential expression of GSK-3α and *β* in tissues suggests that these two isoforms are differentially regulated.[2c] GSK-3 has specific requirements for the recognition of some of its substrates such as GS and tau protein.[3] For example, GS inhibition requires prior phosphorylation by a priming kinase such as casein kinase II to form the motif Ser/T−X−X−X−X−S(P)/T(P) before phosphorylation by GSK-3 is possible.[3a]

GSK-3 regulates GS, the rate-determining enzyme for glycogen synthesis and is of importance in type 2 diabetes. Phosphorylation of GS by GSK-3 results in its deactivation, causing an increase in plasma glucose in type 2 diabetics. Inhibition of GSK-3 would result in an overall state of more active GS, which should lower plasma glucose by increasing glycogen levels. Liver and muscle glycogen synthesis is defective in type 2 diabetics. In addition, the activity of GS itself is also reduced, along with the elevated expression and activity of GSK-3.[4a−c] GSK-3 has been attributed as a negative regulator of insulin synthesis, resulting in impaired glycogen synthesis. Recent studies have demonstrated the in vivo efficacy of GSK-3 inhibitors in ZDF rats as well as the ex vivo effects on human skeletal muscle. These studies have shown that GSK-3 inhibition increases liver glycogen levels, resulting in improved oral glucose disposal and enhanced insulin action of glucose transport in skeletal muscle.[4d,e] In addition, selective inhibition of GSK-3 has been shown to reduce the expression of two key gluconeogenic genes such as glucose-6-phosphatase and phosphoenolpyruvate.[4f]

In mammalian cells, GSK-3α is phosphorylated at serine 21, and GSK-3*β* is phosphorylated at serine 9 by insulin, resulting in their deactivation. This action of insulin is mediated through IRS-2 via PKB/Akt, a serine/threonine kinase located downstream from PI3K.[5b] Glycogen accumulation by the deactivation of GSK-3*β* via an insulin-independent mechanism has also recently been reported. This involves the activation of p90rsk (RSK1 isoform) followed by the activation of ERK1/2 and serine 9 phosphorylation.[7d] In addition, serine 21 in GSK-3α and serine 9 in GSK-3*β* are also physiological substrates of cAMP-dependent protein kinase A (PKA).[6] Besides PKA and PKB, other known negative regulators of GSK-3 are EGF via p90Rsk, PKC, and p70S6.[5a,7] In contrast to inhibitory modulation that occurs via serine phosphorylation, tyrosine phosphorylation (Y216) on the activation loop is known to increase GSK-3 activity. Such activators include ZAK1, Fyn, and transient calcium increases.[8] These endogenous physiological modifiers of GSK-3 tightly regulate GSK-3 activity.

GSK-3 has also been linked to abnormalities associated with Alzheimer's disease via hyperphosphorylation of the microtubule-associated protein tau.[9] Recent studies indicate that the isoform GSK-3*β* facilitates amyloid precursor protein (APP) processing, resulting in the

* Author to whom correspondence should be addressed. Phone: (919) 483-7456. Fax: (919) 483-6053. E-mail: fxt66911@gsk.com.
[†] Department of Medicinal Chemistry.
[‡] Department of Metabolic Diseases.
[§] Department of Computational, Analytical, and Structural Sciences.
[||] Department of Research Bioanalysis and Drug Metabolism.
[⊥] Department of Biochemical and Analytical Pharmacology.

10.1021/jm040063i CCC: $27.50
Published on Web 08/13/2004

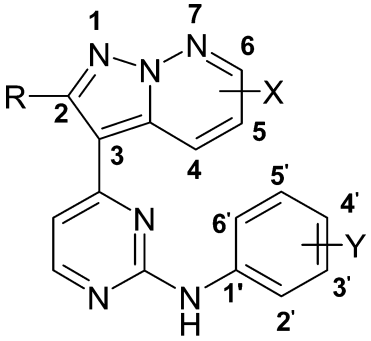

Figure 1.

increased production and aggregation of amyloid-β (Ab) peptides.[10] In addition to its role in metabolic and neurological abnormalities, GSK-3 is also implicated in the regulation of many transcriptional factors. These include cyclic AMP response element binding protein, the nuclear factor of activated T cells, heat shock factor-1, activator protein-1, β-catenin, NF-*k*B, and Myc.[6b,11]

There have been several reports on the regulation of GSK-3 activity involving both genetic methods and small-molecule inhibitors. The conditional overexpression of GSK-3β in mice results in neurodegeneration via hyperphosphorylation of tau in the hippocampal neurons.[12] Antisense targeting of GSK-3 has also been used to inhibit cellular GSK-3 activity.[12] Because genetic techniques can sometimes have spurious effects on cell physiology that are independent of GSK-3, it would be highly desirable to have a specific small-molecule inhibitor of GSK-3 to address its physiological effects. Lithium chloride was one of the early compounds that was found to competitively inhibit GSK-3 with respect to the Mg ion but not substrate or ATP.[14] However, LiCl is not a selective inhibitor of GSK-3 but also has low millimolar inhibitory activity against casein kinase 2, p38 regulated/activated kinase, and MAP-activated protein kinase.[15] Recent reports on the development of small-molecule GSK-3 inhibitors that compete reversibly with ATP have been disclosed. Among these GSK-3 inhibitors are the indirubins, paullones, hymenialdisine, anilinomaleimides, CHIR98023, diaminothiazoles, oxalylpyridines, triazole-4-carboxylic acid derivatives, 1-(4-aminofurazan-3-yl)-5-dialkylaminomethyl-1-H-[1,2,3]-triazole-4-carboxylic acid derivatives, bis-7-azaindolylmaleimides, and pyrazolo[3,4-b]pyridines.[16] In addition, there are reports of non-ATP competitive GSK-3β inhibitors.[17]

The synthetic efforts in our laboratories have focused on the pyrazolo[1,5-*b*]pyridazine screening hit **16** (IC_{50} = 0.019 μM) from the in-house GSK compound collection. The aim was to optimize the kinase selectivity, GSK-3 potency, efficacy, and physiochemical features of **16** by examining the changes in the 2, 3, 5, and 6 positions of the pyrazolo[1,5-*b*]pyridazine core (Figure 1). A search of the literature revealed that most compounds that are potent GSK-3 inhibitors also inhibit cyclin-dependent kinases (CDKs).[18] This was not surprising considering the high degree of homology between the two kinases in the ATP binding site (~86% homology). In light of the fact that CDKs are key regulators of the cell cycle, the complex process by which cells divide,[19] it was highly desirable to avoid inhibiting the CDKs. Due to the activity of screening hit **16** at GSK-3, CDK-2, and CDK-4, the efforts from our laboratories focused initially on dialing out CDK activity using structure-based design and homology modeling. The synthesis and kinase selectivity of these compounds is described herein. In addition, a functional assay of GSK-3 inhibitors showing increased glycogen accumulation in muscle L6 cells will be reported. Furthermore, oral exposure of a representative example will be described briefly, extending the utility of this class of molecules in an in vivo setting.

Chemistry

The general synthesis of substituted pyrimidines (**16**−**37, 57**−**107**) is shown in Scheme 1. Pyridazine **1** was treated with hydroxylamine-*O*-sulfonic acid (HOSA) to provide the intermediate substituted 1-aminopyridazinium salt. The subsequent addition of substituted 3-butyne-2-ones in the presence of a base afforded the 1-pyrazolo[1,5-*b*]pyridazin-3-ylethanones (**2**).[20] The treatment of **2** with dimethylformamide di-*tert*-butylacetal provided substituted (2E)-3-(dimethylamino)-1- pyrazolo[1,5-*b*]pyridazin-3-yl-2-propen-1-ones (**3**), which upon reaction with phenyl guanidines afforded the substituted pyrimidines. The aryl-guanidines **17a**, **18a**, **31a**, and **34a**−**36a** were synthesized using known procedures.[21]

Scheme 1. Synthetic Routes to Targets **16**−**37** and **57**−**107**

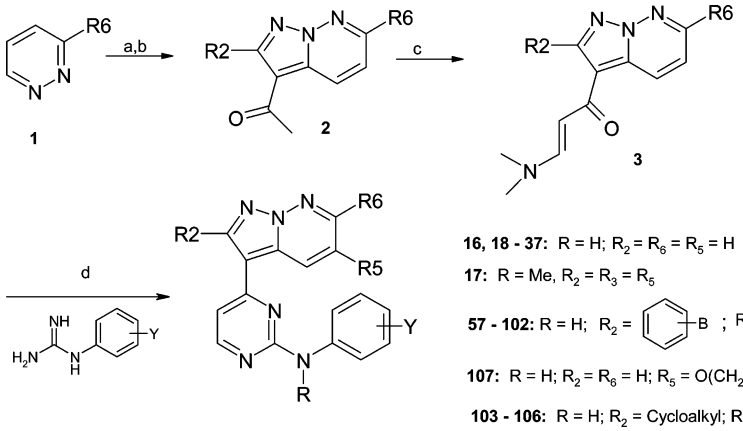

(a) HOSA, aqueous $KHCO_3$, pH 5.0; (b) 3-butyne-2-ones, CH_2Cl_2, r.t.; (c) dimethylformamide di-*tert*-butylacetal, 90 °C; (d) phenyl guanidines.

Table 1. Inhibitory Potencies (IC_{50}) vs Human GSK-3β, CDK-2, and CDK-4

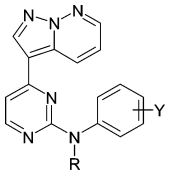

16 - 37

compd	structure (Y)	R	GSK-3 (μM) K_i[a]	CDK-2 (μM)	CDK-4 (μM)
16	H	H	0.019	0.005	0.158
17	H	Me	>19.90	>19.90	nd
18	2-Me	H	6.0	nd	nd
19	3-OMe	H	0.010	0.002	0.063
20	4-CN	H	<0.010 (0.002)	0.001	0.063
21	4-NO_2	H	<0.010 (0.002)	0.022	0.025
22	4-$CH(CH_3)_2$	H	0.031	0.016	1.99
23	4-$CH(C_2H_5)(CH_3)$	H	0.125	0.158	0.316
24	4-$C(CH_3)_3$	H	0.050	0.158	1.99
25	3-OMe, 4-OMe	H	0.012	0.050	0.199
26	3,4-OCH_2O^-	H	<0.010 (0.002)	0.019	0.794
27	3,4-$O(CH_2)_2O$-	H	<0.010 (0.001)	0.006	0.015
28	3-F, 4-F	H	0.010	0.002	nd
29	3,4-$O(CH_2)_3O^-$	H	<0.010 (0.001)	0.006	0.316
30	3-Cl, 4-Cl	H	0.010	0.001	0.199
31	4-Cl, 3-CF_3	H	<0.010 (0.002)	0.012	0.015
32	3-OMe, 5-OMe	H	0.012	0.015	0.019
33	3-OMe, 5-CF_3	H	<0.010 (0.002)	0.015	0.199
34	3-Br, 5-CF_3	H	<0.010 (0.00030)	0.012	0.251
35	3-F, 5-F	H	<0.010 (0.002)	0.001	0.006
36	3-Cl, 5-Cl	H	<0.010 (0.001)	0.316	1.99
37	3-Me, 5-Me	H	<0.010 (0.001)	0.003	1.58

[a] Numbers in parentheses represent K_i values.

Scheme 2. Synthetic Route to Targets **22**−**28**

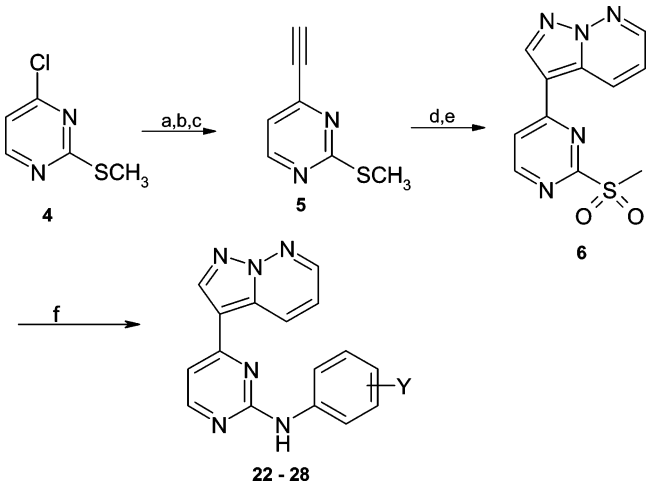

(a) HI; (b) TMS−acetylene, $PdCl_2$, CuI, THF, Et_3N; (c) TBAF/THF; (d) 1-aminopyridazinium iodide, r.t.; (e) *m*-CPBA; (f) anilines, 170 °C, 15 min.

Compounds **22**−**28** (Table 1) were synthesized using the method shown in Scheme 2. The treatment of 4-chloro-2-(methylthio)pyrimidine (**4**) with HI yielded 4-iodo-2-(methylthio)pyrimidine. The subsequent reaction with TMS−acetylene under Sonogashihara conditions,[22] followed by the desilylation of the TMS group with KF, afforded 4-ethynyl-2-(methylthio)pyrimidine (**5**). The treatment of compound **5** with 1-aminopyridazinium iodide in the presence of a base yielded 3-[2-(methylthio)pyrimidin-4-yl]pyrazolo[1,5-*b*]pyridazine, which was subjected to *m*-CPBA, affording sulfone **6**.

Table 2. Inhibitory Potencies (IC_{50}) vs Human GSK-3β, CDK-2, and CDK-4

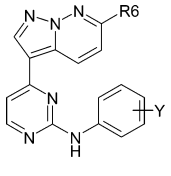

38 - 56

compd	structure (Y)	R6	GSK-3 (μM)	CDK-2 (μM)	CDK-4 (μM)
38	3-CF_3	OH	0.016	0.008	nd
39	3-CF_3	OMe	0.050	0.160	>19.95
40	3-CF_3	OC_2H_5	0.199	1.995	nd
41	3-CF_3	OC_3H_7	0.794	1.26	nd
42	3-OMe	OMe	0.100	0.063	>19.95
43	3-OCF_3	OMe	0.050	0.199	>19.95
44	4-CN	OMe	0.050	0.501	0.158
45	4-NO_2	OMe	0.079	0.020	0.100
46	3-OMe, 5-OMe	OMe	0.125	0.199	>19.95
47	3-OMe, 5-CF_3	OMe	0.199	0.794	>19.95
48	3-OMe, 5-CF_3	OC_2H_5	3.162	>19.95	nd
49	3-CF_3, 5-CF_3	OMe	0.630	>19.95	nd
50	3,4-$O(CH_2)_2O^-$	OMe	0.039	0.100	1.58
51	3-CF_3	Me	<0.010	0.050	0.031
52	4-CF_3	Me	0.050	0.199	nd
53	3-OMe, 5-CF_3	Me	0.010	0.020	0.398
54	3,4-$O(CH_2)_2O^-$	Me	0.010	0.006	0.079
55	3-CF_3	Ph	0.158	2.50	nd
56	3,4-$O(CH_2)_2O^-$	Ph	0.125	>19.95	nd

The sulfonyl group was displaced with substituted anilines to provide the pyrimidines.

The pyrazolopyridazines containing an alkoxy group in the 6 position were synthesized as shown in Scheme 3. The displacement of one of the chloro groups in **7** with alkoxides, followed by reductive heterogenolysis, yielded 3-alkoxypypidazines (**8**). Amination to **8** with HOSA followed by cyclization with 3-butyne-2-one gave **9**. Compound **9** was sequentially treated with dimethylformamide di-*tert*-butylacetal and phenyl guanidines to afford the pyrimidines shown in Table 2 (**38**−**50**).

The pyrimidines (R6 = Ph, Me) were synthesized as shown in Scheme 4. The sequential treatment of 3-chloro-4-substituted pyridazine (**10**) with Pd/C/H_2, HOSA, and 3-butyne-2-one afforded intermediate **11**. The treatment of **11** with dimethylformamide di-*tert*-butylacetal provided the intermediate-substituted (2*E*)-3-(dimethylamino)-1- pyrazolo[1,5-*b*]pyridazin-3-yl-2-propen-1-ones, which upon reaction with phenyl guanidines afforded the substituted pyrimidines in Table 2 (**51**−**56**).

Compound **107** was synthesized from **12** as follows (Scheme 5). The displacement of the 5-chloro group from 4,5-dichloropyridazin-3(2*H*)-one upon treatment with sodium methoxide followed by the removal of the 4-chloro substituent using Pd/C under hydrogen afforded 5-methoxypyridazin-3(2*H*)-one (**13**). The treatment of compound **13** with phosphorus oxychloride followed by the removal of the chloro group gave 4-methoxypyridazine **14**. Compound **14** was sequentially treated with HOSA, butyne-2-one, and dimethylformamide di-*tert*-butylacetal to afford (2*E*)-3-(dimethylamino)-1-(5-methoxypyrazolo[1,5-*b*]pyridazin-3-yl)prop-2-en-1-one (**15**) with the expected regiochemistry of the methoxy group. Compound **15** on treatment with 3-methoxyphenyl guanidine in the presence of potassium carbonate in methoxyethanol afforded 4-[5-(2-methoxyethoxy)pyra-

Scheme 3. Synthetic Route to Targes **38**−**50**

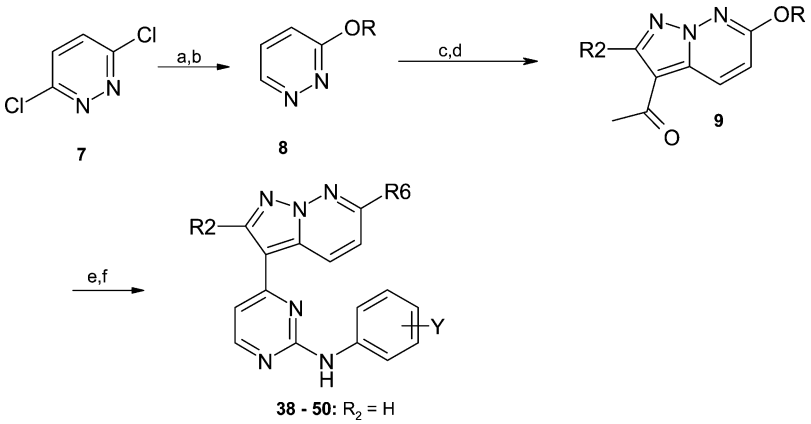

(a) Sodium alkoxide, r.t.; (b) H_2, Pd/C; (c) HOSA, aqueous $KHCO_3$, pH 8.0; (d) 3-butyne-2-ones, CH_2Cl_2, r.t.; (e) dimethylformamide di-*tert*-butylacetal, 90 °C; (f) phenyl guanidines (**16a**−**21a**, **29a**−**37a**).

Scheme 4. Synthetic Route to Targets **51**−**56**

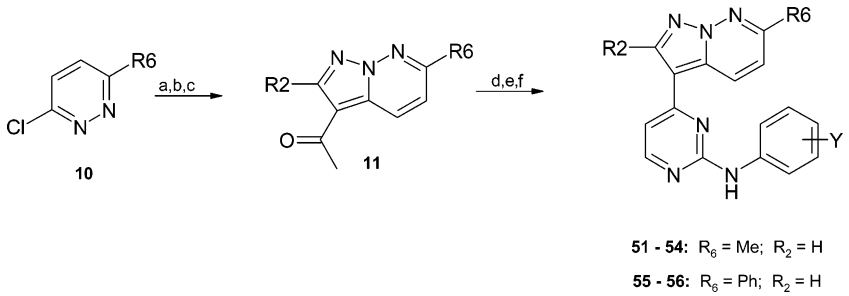

(a) Sodium alkoxide, r.t; (b) H_2, Pd/C; (c) HOSA, aqueous $KHCO_3$, pH 5.0; (d) 3-butyne-2-ones, CH_2Cl_2, r.t.; (e) dimethylformamide di-*tert*-butylacetal, 90 °C; (f) phenyl guanidines.

Scheme 5. Synthetic Route to Target **107**

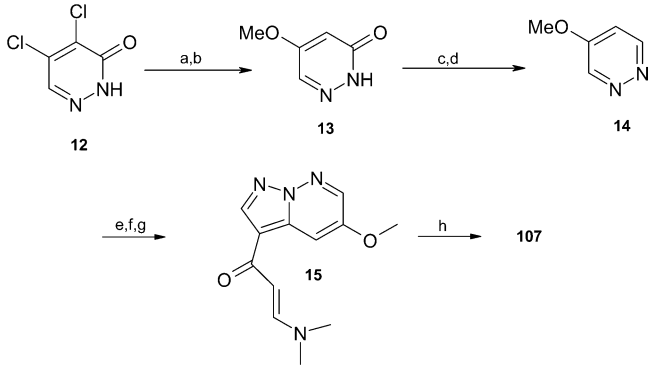

(a) Sodium methoxide, MeOH; (b) H_2, Pd/C; (c) $POCl_3$ (d) H_2, Pd/C; (e) HOSA, aqueous $KHCO_3$, pH 5.0; (f) 3-butyne-2-ones, CH_2Cl_2, r.t.; (g) dimethylformamide di-*tert*-butylacetal, 90 °C; (h) *N*−(3-methoxyphenyl)guanidine, methoxyethanol.

zolo[1,5-*b*]pyridazin-3-yl]-*N*−(3-methoxyphenyl)pyrimidin-2-amine (**107**).

Results and Discussion

In the process of developing selective GSK-3 inhibitors, we identified compound **16** (GSK-3 IC_{50} = 0.019 μM) to be a potential starting point in the program. The IC_{50} values are the mean of two or three inhibition assays with a 2-fold standard deviation. The K_I values are also the mean of two or three inhibition assays with an error bar of 12%. From Table 1, it can be seen that compound **16** is also a very potent inhibitor of CDK-2 (IC_{50} = 0.005 μM) and CDK-4 (IC_{50} = 0.158 μM). To reduce CDK activity selectively, it was important to consider the key residues that were involved in the binding of **16** to both GSK-3 and CDK-2. To determine the necessity of the NH in binding to the backbone of the ATP binding loop, we synthesized compounds **17** (IC_{50} >19.9 μM) and **18** (IC_{50} = 6.0 μM). The addition of an *N*-methyl group destroyed the activity at GSK-3. Also, having an *ortho*-methyl substituent resulted in a dramatic decrease in activity, suggesting that the NH formed an important hydrogen-bonding interaction with the enzyme.

In the absence of an X-ray structure of **16**, we used information on the published X-ray crystal structure complexed with FRATtide[16j] and an in-house cocrystal structure of pyrazolo[3,4-*b*]pyridazine[16k] to elucidate the binding mode of **16**. Compound **16** was also docked into an in-house crystal structure of cyclin A/CDK-2[16n]. The results from the automated docking of **16** in GSK-3 and CDK-2 are shown in Figure 2. As can be seen in Figure

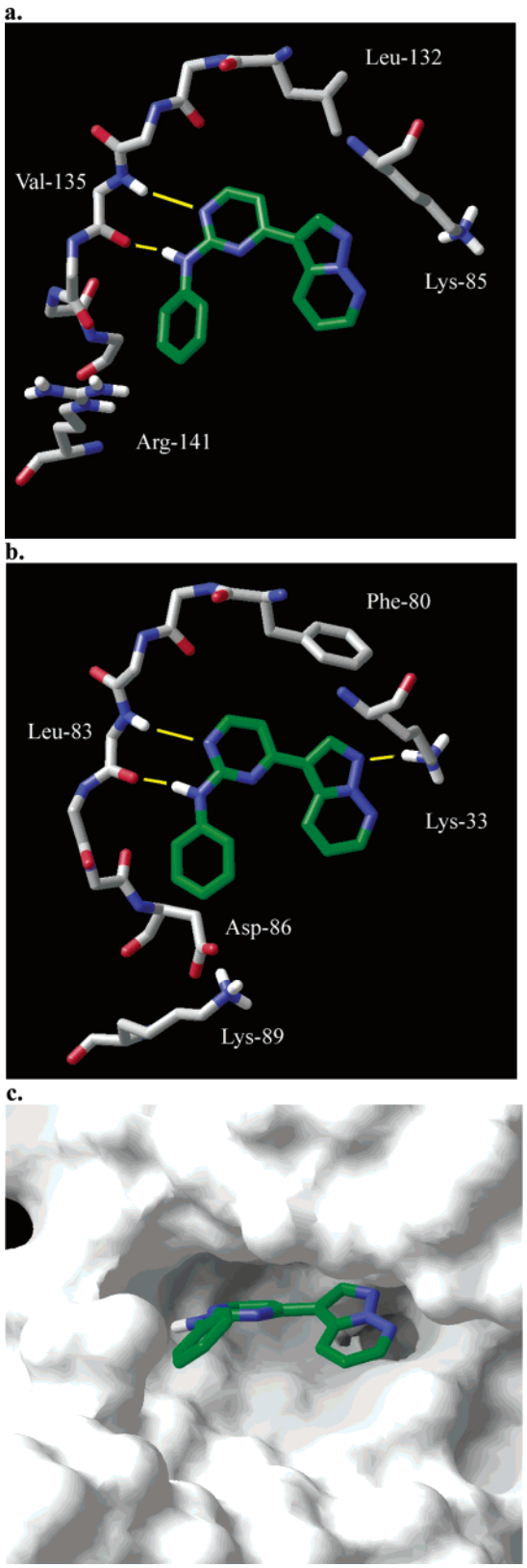

Figure 2. Binding mode of compound **16** in the ATP sites of GSK-3β (a) and CDK-2 (b). The backs of the pockets are shown at the top. Key H bonds between **16** and the active site are highlighted by yellow lines. (c) Surface of active site of GSK-3β.

2, the NH and the adjacent nitrogen in the pyrimidine ring of the ligand make hydrogen-bonding interactions with the hinge region of both kinases. In GSK-3β (Figure 2a), it is Val 135, whereas in CDK2 (Figure 2b), it is Leu 83. A key difference in these binding sites is located in the back pocket, where there is a leucine (Leu 132) in GSK-3 and a phenylalanine (Phe 80) in CDK-2. The hydrogen at the 2 position in compound **16** appeared to favorably interact with the face of the phenyl group of Phe 80 in the CDK-2 model. The two models also suggested a slightly different interaction with the conserved lysines. The pyrazolopyridazine nitrogens appeared to be able to make a direct hydrogen bond with the hydrogens on the protonated nitrogens on Lys 33 in CDK-2, whereas in GSK-3, they appear to interact with the slightly electropositive chain of the residue (Lys 85). The front of the binding sites was largely solvent exposed and appeared to be more open in the GSK-3 model.

The monosubstituted aniline analogues (Table 1, compds **19**−**24**) were potent inhibitors of GSK-3, with a tendency to be slightly less potent at CDK-2 when compared to unsubstituted parent **16**. On the basis of our binding model highlighted in Figure 2b, increasing the steric bulk at the 4′ position of compound **16** docked into CDK-2 suggested that steric repulsion with amino acid Asp 86 (CDK-2) and amino acid residue Lys 89 (CDK-4) could potentially provide us with selectivity over CDK-2 and CDK-4. SAR at this position (compounds **22**−**24**) was consistent with our binding model with improvements in selectivity versus CDK-2. From Table 1, it can be seen that there was a 2-fold loss in potency against GSK-3 on going from unsubstituent parent **16** to *tert*-butyl analogue **24**, but there were correspondingly greater losses in potency in CDK-2 (31-fold) and CDK-4 (12-fold).

The influence of the substitution pattern at the anilino moiety on the inhibitory activity of the compounds was also examined. The addition of 3′,4′- and 3′,5′-disubstituted analogues was considered (compds **25**−**37**, Table 1). From modeling studies, the substituents at the 3′ and 4′ positions were well placed for a charged interaction with positively charged Arg 141 (GSK-3) or negatively charged Asp 86 (CDK-2). There was no overriding electronic component to the activity at these positions. Compounds with electron-donating and electron-withdrawing groups in the anilino substituent resulted in very potent inhibitors of GSK-3 (compare **25** vs **28** and **30**, and **35** and **36** vs **37**). Also, potency gains in the disubstituted analogues of compound **16** were not as dramatic, suggesting that any gain in binding due to favorable substituent interactions may be compromised by the energy needed for the desolvation process. Additionally, the incorporation of electron-rich substituents, such as in compounds **19** and **25**−**29**, provided no selectivity over CDK-2 in spite of the potential for a favorable interaction with positively charged Arg 141 (GSK-3β) and an unfavorable electronic/steric repulsion with negatively charged Asp 86 (CDK-2). Such favorable/unfavorable electronic interactions have been fruitful in gaining selectivity over CDK-2 for some recently disclosed GSK-3 inhibitors.[16k,m] 3′,5′-Dichloro analogue **36** was found to be the most selective inhibitor of GSK-3 (Table 1), with over 30-fold selectivity over CDK-2 and greater than 190-fold selectivity over CDK-4. However, compound **36** was apparently found to be the least efficacious analogue in terms of glycogen accumulation. Interestingly, compound **37** was also

found to be one of the most potent compounds in this series. Favorable hydrophobic binding and the absence of an unfavorable desolvation penalty might explain the increase in potency of **37**.

On the basis of our GSK-3 inhibitor binding model (Figure 2a), there was the potential of having substituents at the 6 position that might provide opportunities to improve the selectivity and physiochemical properties of these inhibitors. For example, hydroxyl compound **38** was found to be a potent inhibitor of GSK-3. Increasing the steric bulk at the hydroxyl, as in compounds **39**−**41**, **47**, and **48**, resulted in a loss in potency. This loss was more pronounced with the CDKs. Molecular modeling calculations suggested that the low-energy conformation of the alkoxy points toward the N 7 nitrogen. Such an orientation would have the alkoxy group bumping into Phe 67 in the p loop of GSK-3 and would presumably result in a considerable loss of potency. The addition of a bulky alkoxy substituent at the 5 position, as in analogue **107** (GSK-3 IC_{50} = 0.080 μM), resulted in a potent GSK-3 inhibitor. This was consistent with our binding model, which orients the 5 position into an open space within the enzyme active site that appeared to accommodate large substituents. In the alkoxy series, compound **49** was found to be the most GSK-3-selective inhibitor versus CDK-2. 6-methyl analogues **51**−**54** were well tolerated (compound **53** vs **33** and **54** vs **29**) and generally more potent compared to the alkoxy derivatives (compound **51** vs **39** and **53** vs **47**). The 6-methyl analogues were not found to be selective over CDK-2. 6-Phenyl analogues **55**−**56** showed a reduction in potency similar to that of the 6-alkoxy compounds. However, compound **56** was found to be the most selective 6-substituted analogue.

Our binding model indicated that substituents in the 2 position of the pyrazolopyridine core would project in the direction of the gatekeeper. As observed in Figure 2a and b, the gatekeeper in CDK-2 is sterically more demanding (Phe 80) compared to that in GSK-3β (Leu 132). To take advantage of the differences in steric congestion and possibly to provide potency/selectivity over CDKs, we made compounds with substitutions at the 2 position. In addition, mix-and-match combinations with a set of anilino compounds, including the incorporation of the 6-methyl substituent, were made (Table 3). As can be seen from Table 3, 2-phenyl compound **57** (GSK-3 IC_{50} = 0.010 μM) was a potent inhibitor of GSK-3 with a selectivity of about 400-fold over CDK-2. The addition of a 3′-trifluoromethyl phenyl substituent (compound **58**, GSK-3 IC_{50} = 0.012 μM) gave an extremely selective (>1600-fold over CDK-2) and potent inhibitor of GSK-3. The disubstituted anilino analogues (**59**−**62**) also showed a similar trend. The additional gain in selectivity with substituted anilino groups versus compound **57** indicates that the accommodation of the anilino substituents in the narrow cleft is less favorable in CDK-2 than in GSK-3. To explore the steric requirements at the gatekeeper region, we made various 2-aryl analogues. The addition of a 2-(4-fluorophenyl) substituent (compounds **63**−**67**) provided highly potent and selective compounds. Interestingly, the addition of the fluoro group at the 4 position of **57** (compound **63**) provided greater selectivity against CDK-2. The incorporation of the 6-methyl group in the 2-phenyl and 2-(4-fluoro phenyl) analogues (compounds **87**−**91**, **98**−**102**) also provided potent and selective inhibitors of GSK-3. As can be seen from Table 3 (compounds **68**−**72**), the addition of a 4-methoxyphenyl group was found to be detrimental, with a drop of between 500- and 3000-fold in activity (**57**−**62** vs **68**−**72**). The incorporation of a 3- or 4-trifluoromethylphenyl group at the 2 position (compounds **73**−**81**) led to a greater loss in GSK-3 activity. A similar trend was observed for the 6-methyl analogues having a 4-trifluoromethylphenyl group at the 2 position (compounds **96**−**97**). The incorporation of a 6-methyl substituent along with the 3-trifluoromethyl phenyl group (compounds **92**−**95** vs **78**−**81**)

Table 3. Inhibitory Potencies (IC_{50}) vs Human GSK-3β and CDK-2

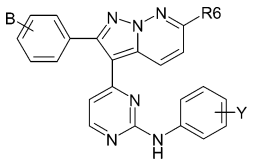

57 - 102

compd	structure (Y)	R6	B	GSK-3 (μM) K_i[a]	CDK-2 (μM)
57	H	H	H	0.010	3.98
58	3-CF_3	H	H	0.012	>19.95
59	3-F, 4-F	H	H	0.010	>19.95
60	3-F, 5-F	H	H	0.011	>19.95
61	4-Cl, 3-CF_3	H	H	0.020	>19.95
62	3,4-O$(CH_2)_2$O-	H	H	<0.010 (0.002)	>19.95
63	H	H	4-F	0.020	>19.95
64	3-CF_3	H	4-F	0.020	>19.95
65	3-F, 4-F	H	4-F	0.025	>19.95
66	4-Cl, 3-CF_3	H	4-F	0.040	>19.95
67	3,4-O$(CH_2)_2O^-$	H	4-F	0.010	>19.95
68	H	H	4-OMe	5.01	>19.95
69	3-CF_3	H	4-OMe	31.6	>19.95
70	3-F, 4-F	H	4-OMe	7.94	>19.95
71	4-Cl, 3-CF_3	H	4-OMe	31.0	>19.95
72	3,4-O$(CH_2)_2O^-$	H	4-OMe	5.01	>19.95
73	H	H	4-CF_3	>31.6	>19.95
74	3-CF_3	H	4-CF_3	>31.6	>19.95
75	3-F, 4-F	H	4-CF_3	>31.6	>19.95
76	3,4-O$(CH_2)_2O^-$	H	4-CF_3	>31.6	>19.95
77	4-Cl, 3-CF_3	H	4-CF_3	>31.6	>19.95
78	H	H	3-CF_3	0.158	>19.95
79	3-F, 4-F	H	3-CF_3	0.316	>19.95
80	3,4-O$(CH_2)_2$O-	H	3-CF_3	0.050	>19.95
81	4-Cl, 3-CF_3	H	3-CF_3	1.0	>19.95
82	H	H	4-Cl	1.25	>19.95
83	3-CF_3	H	4-Cl	2.51	>19.95
84	3-F, 4-F	H	4-Cl	1.0	>19.95
85	4-Cl, 3-CF_3	H	4-Cl	3.98	>19.95
86	3,4-O$(CH_2)_2O^-$	H	4-Cl	0.796	>19.95
87	H	Me	H	0.050	>19.95
88	3-CF_3	Me	H	0.040	>19.95
89	3-F, 4-F	Me	H	0.031	>19.95
90	4-Cl, 3-CF_3	Me	H	0.100	>19.95
91	3,4-O$(CH_2)_2O^-$	Me	H	0.032	>19.95
92	H	Me	3-CF_3	0.794	>19.95
93	3-F, 4-F	Me	3-CF_3	1.58	>19.95
94	4-Cl, 3-CF_3	Me	3-CF_3	0.630	>19.95
95	3,4-O$(CH_2)_2O^-$	Me	3-CF_3	0.158	5.0
96	H	Me	4-CF_3	>31.6	>19.95
97	3,4-O$(CH_2)_2O^-$	Me	4-CF_3	>31.6	>19.95
98	H	Me	4-F	0.025	>19.95
99	3-CF_3	Me	4-F	0.025	>19.95
100	3-F, 4-F	Me	4-F	0.016	>19.95
101	3,4-O$(CH_2)_2O^-$	Me	4-F	0.016	>19.95
102	4-Cl, 3-CF_3	Me	4-F	0.050	>19.95

[a] Numbers in parentheses represent K_i values.

Table 4. Inhibitory Potencies (IC_{50}) vs Human GSK-3β and CDK-2

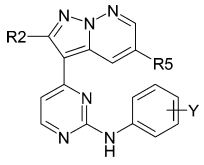

103 - 107

compd	structure (Y)	R5	R2	GSK-3 (μM)	CDK-2 (μM)
103	H	H		19	3.98
104	3-F, 4-F	H		23	>19.95
105	H	H	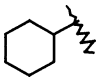	>19.95	>19.95
106	3-F, 4-F	H	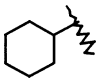	>19.95	>19.95
107	3-OMe	$O(CH_2)_2OMe$	H	0.080	>19.95

resulted in the maintenance of potency at GSK-3. Interestingly, a smaller 4-chlorophenyl substituent at the 2 position was better accommodated in the binding pocket with a smaller drop (80−400-fold) in potency against GSK-3 than the corresponding 4-trifluoromethyl analogues (compounds **57**−**62** vs **83**−**86**). The SAR that was generated from the substituents on the 2-phenyl ring suggests that smaller substituents such as fluoro and chloro are easily accommodated at the 4 position.

An incorporation of groups at the 2 position other than aryl was also made (compounds **103**−**106**). The 2-cyclopropyl and the bulkier 2-cyclohexyl analogues were weak inhibitors of GSK-3, suggesting that the binding space at the 2 position may be unique for the accommodation of a phenyl substituent.

Although a thorough pharmacokinetic analysis was not done, a representative example was shown to exhibit very good oral exposure in an abbreviated pk setting in mice. Compound **99** dosed at 10 mg/kg was found to have an AUC (0−6 h) = 2.619 h·μg/mL and a C_{max} = 0.558 μg/mL. The concentration in the final sample was 0.435 mg/mL, indicating that the total AUC would have been significantly greater than that determined for the 6-h sampling interval. This compound had moderate permeability in the MDCK cell line (P_{app} = 66 nm/s).

Cellular Activities

To measure the functional effects of GSK-3 inhibition, we evaluated compounds on the basis of their ability to increase glycogen deposition in a rat skeletal muscle L6 myoblast cell line. The EC_{50} and percent response values in Table 5 are the means of three inhibition assays; individual data points in each experiment were within 15 and 6% error, respectively. Most compounds were fairly active in the L6 cell line. Analogue work on the HTS hit **16** (EC_{50} = 2.9 μM) allowed for improvements in cellular potency and enhanced glycogen accumulation. In Table 5, representative examples from the pyrazolo[1,5-*b*]pyridazine class of GSK-3 inhibitors are shown. With respect to insulin response (100%), the glycogen accumulation with GSK-3 inhibitors, with the exception of **16** and **36**, ranged from 27 to 78%, indicating that this class of inhibitors showed not only in vitro enzyme inhibition but also functional activity in the relevant L6 cell line.

Table 5. Cell Efficacy and Functional Response for Selected Compounds

compd	EC_{50} (μM)	% response[a]
16	2.9	18
19	1.3	56
25	1.5	27
27	0.8	27
31	1.0	38
33	1.2	43
35	1.0	47
36	1.0	14
37	1.8	58
57	1.6	78
58	2.1	76
59	4.2	69
64	2.8	35
87	3.6	56
89	3.4	66
99	6.8	38

[a] Maximal effect of compound vs insulin effect toward glycogen accumulation.

Conclusions

Starting with a GSK-3 inhibitor that was equipotent against CDK-2, we used analogue design and modeling work to dial out CDK potency by studying the effects of substution at the 2, 3, 5, and 6 positions of the pyrazolopyridazine core. The knowledge of the initial modifications that led to the selectivity in the 3 position was applied to analogue design in the 2 and 6 positions. Although some degree of selectivity was achieved in the 6 position, modifications in the 2 position led to the most selective GSK-3 inhibitors having virtually no activity against the CDKs. Further modifications of HTS hit **16** afforded compounds with improved cell potency and functional response with respect to the same properties in insulin. In addition, a representative example from this class showed good oral exposure. Since many of the GSK-3 inhibitors reported in the literature also possess potent CDK activity, this work for the first time provides direction in the kinase area to solve this extremely difficult problem by making use of key residues in the back pocket to afford extremely CDK-2-selective GSK-3 inhibitors. Combined with their good cell efficacy and functional response, this series represents a viable lead in the study of the pharmacological effects of GSK-3 inhibition.

Experimental Section

Chemistry. General Methods. Melting points were determined using a Thomas−Hoover melting point apparatus and are uncorrected. Unless stated otherwise, reagents were obtained from commercial sources and were used directly. Reactions involving air- or moisture-sensitive reagents were carried out under a nitrogen atmosphere. If not specified, reactions were carried out at ambient temperature. Silica gel (EM Science, 230−400 mesh) was used for chromatographic purification unless otherwise indicated. Anhydrous solvents were obtained from Aldrich (Sure Seal). ^{1}H NMR spectra were recorded on a Varian spectrometer; chemical shifts are reported in ppm relative to TMS. The following abbreviations are used to describe peak patterns when appropriate: b = broad, s = singlet, d = doublet, t = triplet, q = quartet, and m = multiplet. High-performance liquid chromatography (HPLC)

was performed on a Beckman 126 chromatograph with a Beckman 166 UV detector (monitoring at 215 nm) with a Rainin Dynamax-60A column using a gradient consisting of 20:80 A/B to 10:90 A/B over 20 min, where A = 1% aqueous trifluoroacetic acid (TFA) and B = 1% TFA in CH_3CN. Elemental analyses, performed by Atlantic Microlab, Inc., Norcross, GA, were within 0.4% of the theoretical values calculated for C, H, and N. For compounds that did not undergo elemental analysis, purity was determined by using two different methods (method A: MeOH/H_2O from 0 to 100%; method B: CH_3CN/H_2O from 10 to 100%). Compounds were found to be >95% pure by both methods A and B unless otherwise as stated in the experimental specifications.

General Procedure for the Preparation of Guanidine Nitrates. To a solution of aniline (20 mmol) in ethanol (15 mL) was added 1.8 mL (20 mmol) of conc nitric acid followed by a 50% aqueous solution of cyanamide (2.52 mL, 30 mmol)). The reaction mixture was then heated under reflux for 16 h. The reaction was cooled to 0 °C followed by the addition of ether (100 mL). The contents were then refrigerated overnight, and the resulting solid was filtered, affording the product in 70−80% yield.

General Procedure for the Preparation of Compounds 16−21, and 29−37. a. 1-Pyrazolo[1,5-*b*]pyridazin-3-ylethanone. To a solution of hydroxylamine-*O*-sulfonic acid (42 g, 375 mmol) neutralized with 2.5 M potassium bicarbonate to pH 5 was added pyridazine (20 g, 250 mmol) at 70 °C over 15 min. The reaction was stirred at 70 °C for 2 h followed by cooling to room temperature. After neutralization of the reaction mixture to pH 8, but-3-yn-2-one (8.5 g, 125 mmol) in 500 mL of dichloromethane and 26 g (468 mmol) of potassium hydroxide were added, and the contents was stirred at room temperature overnight. The reaction was extracted with dichloromethane (200 × 3), and the combined organic layer was washed with brine and then dried over magnesium sulfate. The removal of the solvent under vacuum and purification by column chromatography with hexane/ethyl acetate (4:1) afforded 23 g of product as a brown solid in 57% yield. ^{1}H NMR (300 MHz, DMSO-d^6) δ: 8.79 (s, 1H), 8.71 − 8.64 (m, 2H), 7.60 (dd, J = 4.5, 4.6 Hz, 1H), 2.56 (s, 3H). MS (ESI) $(M + H)^+$ 162

b. (2*E*)-3-(Dimethylamino)-1-pyrazolo[1,5-*b*]pyridazin-3-ylprop-2-en-1-one. To 1-Pyrazolo[1,5-*b*]pyridazin-3-ylethanone (4.5 g, 27.9 mmol) in 10 mL of DMF was added *N*,*N*-dimethylformamide di-*tert*-butyl (17.0 mL, 83.7 mmol), and the contents was heated to 100 °C for 3 h. After removal of the solvent under vacuum, ether was added, and the mixture was kept at 4 °C overnight. Filtration gave 6.03 g of product as a brown solid in quantative yield. ^{1}H NMR (300 MHz, DMSO-d^6) δ: 8.76 (d, J = 8.6 Hz, 1H), 8.72 (s, 1H), 8.59 (m, 1H), 7.71 (d, J = 12.2 Hz, 1H), 7.44 (dd, J = 4.4, 4.6 Hz, 1H), 5.87 (d, J = 12.4 Hz, 1H), 3.15 (s, 3H), 2.95 (s, 3H). MS (ESI) $(M + H)^+$ 217.

c. General Procedure for the Preparation of Compounds 16−21 and 29−37. To (2*E*)-3-(dimethylamino)-1-pyrazolo[1,5-*b*]pyridazin-3-ylprop-2-en-1-one (0.2 g, 0.926 mmol) in methoxyethanol (5.0 mL) were added solid potassium carbonate (0.255 g, 1.852 mmol) and guanidine (1.20 mmol). The contents were refluxed overnight, and the crude reaction mixture was purified over silica gel using ethyl acetate/hexane as the eluent to afford the desired product in 50−70% yield.

***N*-methyl-*N*-phenyl-4-pyrazolo[1,5-*b*]pyridazin-3-ylpyrimidin-2-amine (17).** This compd was prepared following the general procedure using *N*-methyl-*N*-phenylguanidine nitrate. ^{1}H NMR (300 MHz, DMSO-d^6) δ: 8.86 (s, 1H), 8.55 (s, 1H), 8.44 (d, J = 5.2 Hz, 1H), 8.26 (d, J = 7.8 Hz, 1H), 7.55−7.17 (m, 7H), 3.57 (s, 3H). Elemental analysis was done for C, H, and N.

General Procedure for the Preparation of Compounds 22−28. a. 4-Iodo-2-(methylthio)pyrimidine. To an aqueous solution of 56% HI in water (140 mL) was added 4-chloro-2-(methylthio) pyrimidine (25 g, 155 mmol). The contents was stirred at room temperature for 12 h in the dark. Extraction with dichloromethane (500 mL) was followed by the subsequent washing of the organic phase with a 10% solution of sodium bisulfite (200 mL) and saturated sodium bicarbonate. The organic layer was then dried with magnesium sulfate and concentrated under vacuum to afford 27 g (69%) of a colorless oil, which was taken directly to the next step. ^{1}H NMR (300 MHz, DMSO-d^6) δ: 8.23 (d, J = 5.3 Hz, 1H), 7.73 (d, J = 5.3 Hz, 1H), 2.51 (s, 3H).

b. 4-Ethynyl-2-(methylthio)pyrimidine. To a solution of the iodo compound (27.09 g, 107 mmol) was added triethylamine (18.76 g, 134 mmol), cuprous iodide (1.02 g, 5.35 mmol) and palladium chloride bis-triphenylphosphine (2.25 g, 3.21 mmol). To the reaction mixture was slowly added TMS−acetylene (18.86 mL, 134 mmol), and the contents was stirred at room temperature for 16 h. The reaction mixture was diluted with hexanes, and the solids were filtered off. The concentrated filtrate gave 28.0 g of the silylated intermediate. To the crude silylated intermediate (28.0 g, 128 mmol) in methanol (90 mL) was added potassium fluoride (7.42 g, 128 mmol), and the reaction contents was stirred at room temperature for 10 min. Concentration under vacuum followed by column chromatography over silica gel with ethyl acetate/hexane (2:8) gave 7.8 g (48%) of a brown solid. ^{1}H NMR (300 MHz, DMSO-d^6) δ: 8.70 (d, J = 5.1 Hz, 1H), 7.36 (d, J = 5.1 Hz, 1H), 4.82 (s, 1H), 2.52 (s, 3H). MS (ESI) $(M + H)^+$ 151.

3-[2-(methylthio)pyrimidin-4-yl]pyrazolo[1,5-*b*]pyridazine. To a solution of the iodonium salt (15.0 g, 67 mmol) in dichloromethane (200 mL) was added 4-ethynyl-2-(methylthio)pyrimidine **(**5.02 g, 33.5 mmol) and potassium hydroxide (9.39 g, 167.5 mmol). The reaction mixture was stirred for 20 h at room temperature, and the layers were separated. The organic layer was dried with magnesium sulfate and then separated by column chromatography over silica gel with ethyl acetate/hexane (1:1) to afford 15.3 g (63%) of the product as a brown solid. ^{1}H NMR (300 MHz, DMSO-d^6) δ: 8.96 (s, 1H), 8.94 (m, 1H), 8.66 (m, 1H), 8.61 (d, J = 5.3 Hz, 1H), 7.72 (d, J = 5.3 Hz, 1H), 7.55 (m, 1H), 2.63 (s, 3H). MS (ESI) $(M + H)^+$ 244.

3-[2-(Methylsulfonyl)pyrimidin-4-yl]pyrazolo[1,5-*b*]-pyridazine. To a solution of the thiol (1.0 g, 4.10 mmol) in dichloromethane (70 mL) was added *m*-perchlorobenzoic acid (2.44 g, 10.25 mmol). After stirring for an hour, the reaction mixture was washed with 10% sodium bisulfite followed by a saturated sodium bicarbonate solution. The organic phase was dried with magnesium sulfate and concentrated under vacuum to afford 1.1 g (88%) of the product. ^{1}H NMR (300 MHz, DMSO-d^6) δ: 9.14 (s, 1H), 9.04 (s, 1H), 8.93 (m,1H), 8.74 (m, 1H), 7.67 (m, 1H), 3.53 (s, 3H). MS (ESI) $(M + H)^+$ 276.

General Procedure for the Preparation of Compounds 22−28. To 3-[2-(methylsulfonyl)pyrimidin-4-yl]pyrazolo[1,5-*b*]-pyridazine (0.1 g, 0.363 mmol) was added the substituted anilines (3.63 mmol), and the contents was heated at 170 °C for 15 min. After cooling to room temperature, methanol was added, and the resulting solid was filtered and then washed with methanol. Column chromatography with ethyl acetate/hexane afforded the desired product in 60−70% yield.

***N*−(4-Isopropylphenyl)-4-pyrazolo[1,5-*b*]pyridazin-3-ylpyrimidin-2-amine (22).** This compound was prepared following the general procedure using 4-isopropylaniline. ^{1}H NMR (300 MHz, DMSO-d^6) δ: 9.46 (s, 1H), 9.16 (d, J = 8.8 Hz, 1H), 8.97 (s, 1H), 8.87 (s, 1H), 8.43 (d, J = 5.1 Hz, 1H), 7.63 (d, J = 7.4 Hz, 2H), 7.33 (d, J = 5.1 Hz, 1H), 7.20 (d, J = 7.4 Hz, 2H), 2.89 (m, 1H), 1.21 (d, J = 6.9 Hz, 6H). Elemental analysis was done using method A.

3-(2-{[3-(Trifluoromethyl)phenyl]amino}-4-pyrimidinyl)pyrazolo[1,5-*b*]pyridazin-6-ol (38). To a solution of (0.5 g, 1.29 mmol) of compound **39** was added morpholine (10 mL), and the contents was heated at 120 °C for 14 h. After cooling, the solvents were evaporated under vacuum, and the crude product was purified over silica gel using dichloromethane/methanol (95:5) to afford 0.385 g (80%) of the title compound as a pale-yellow solid. ^{1}H NMR (300 MHz, DMSO-d^6) δ: 9.93 (s, 1H), 8.97 (d, J = 9.6 Hz, 1H), 8.65 (s, 1H), 8.53 (d, J = 5.4 Hz, 1H), 8.32 (s, 1H), 8.01 (d, J = 8.1 Hz, 1H), 7.58 (dd, J = 8.1 and 7.8 Hz, 1H), 7.41 (d, J = 5.4 Hz, 1H), 7.33 (d, J = 7.8

Hz, 1H), 7.01 (d, J = 9.6 Hz, 1H). Elemental analysis was performed for C, H, and N.

4-[6-(Methyloxy)pyrazolo[1,5-*b*]pyridazin-3-yl]-*N*-[3-(trifluoromethyl)phenyl]-2-pyrimidinamine (39). 1-[6-(Methoxy)pyrazolo[1,5-*b*]pyridazin-3-yl]ethanone (39a). In a similar manner to that described in the general procedure for compounds **16**−**21** and **29**−**37** (method a), we obtained the title compound from 3-methoxypyridazine as a brown solid. ^{1}H NMR (300 MHz, $CDCl_3$) δ: 8.58 (d, J = 9.4 Hz, 1H), 8.26 (s, 1H), 6.96 (d, J = 9.4 Hz, 1H), 4.14 (s, 3H). MS (ESI) $(M + H)^+$ 192.

(2*E*)-3-(Dimethylamino)-1-[6-(methoxy)pyrazolo[1,5-*b*]-pyridazin-3-yl]-2-propen-1-one (39b). In a similar manner to that described in the general procedure for compounds **16**−**21** and **29**−**37** (method b), we obtained **39b** as a brown solid from **39a**. ^{1}H NMR (300 MHz, DMSO-d^6) δ: 8.57 (d, J = 9.4 Hz, 1H), 8.51 (s, 1H), 7.67 (d, J = 12.3 Hz, 1H), 7.08 (d, J = 9.4 Hz, 1H), 5.80 (d, J = 12.3 Hz, 1H), 4.06 (s, 3H), 3.14 (br, 3H), 2.92 (br, 3H). MS (ESI) $(M + H)^+$ 247.

4-[6-(Methyloxy)pyrazolo[1,5-*b*]pyridazin-3-yl]-*N*-[3-(trifluoromethyl)phenyl]-2-pyrimidinamine (39). In a similar manner to that described in the general procedure for compounds **16**−**21** and **29**−**37** (method c), we obtained **39** from **39b** as a brown solid. ^{1}H NMR (300 MHz, DMSO-d^6) δ: 9.96 (s, 1H), 9.03 (d, J = 9.6 Hz, 1H), 8.74 (s, 1H), 8.55 (d, J = 5.4 Hz, 1H), 8.30 (s, 1H), 8.00 (d, J = 8.0 Hz, 1H), 7.58 (t, J = 8.0 Hz, 1H), 7.44 (d, J = 5.4 Hz, 1H), 7.33 (d, J = 8.0 Hz, 1H), 7.17 (d, J = 9.6 Hz, 1H), 4.04 (s, 3H). Elemental analysis was performed for C, H, and N.

4-[6-(Ethyloxy)pyrazolo[1,5-*b*]pyridazin-3-yl]-*N*-[3-(trifluoromethyl)phenyl]-2-pyrimidinamine (40). 3-Chloro-6-(ethyloxy)pyridazine (40a). To a solution of (5 g, 33.6 mmol) 3,6-dichloropyridazine in 60 mL of dry ethanol was added 13.1 mL (35.1 mmol) of 21% sodium ethoxide in ethanol at 0 °C. The reaction was stirred at room temperature for 3.5 h. The solvent was removed, and the residue was redissolved in water. The aqueous phase was extracted with dichloromethane, and the combined organic phase was washed with brine and dried over magnesium sulfate. The removal of the solvent gave 5.0 g of the product as a yellow solid in 94% yield. ^{1}H NMR (300 MHz, $CDCl_3$) δ: 7.38 (d, J = 9.1 Hz, 1H), 6.98 (d, J = 9.1 Hz, 1H), 4.57 (q, J = 7.1 Hz, 2H), 1.47 (t, J = 7.1 Hz, 3H). MS (ESI) $(M + H)^+$ 159.

3-(Ethyloxy)pyridazine (40b). A mixture of 15.5 g (98 mol) of 3-chloro-6-(ethyloxy)pyridazine in 150 mL of methanol with 1.5 g of 10% palladium on carbon was hydrogenated under 50 psi overnight. The catalyst was filtered, and the solvent was removed. The residue was redissolved in 300 mL of dichloromethane, and 9 g (107 mol) of sodium bicarbonate was added. The mixture was stirred at room temperature for 30 min and was dried over magnesium sulfate. The removal of solvent followed by column chromatography with hexane/ethyl acetate (2:1) gave 9.7 g of product in 80% yield. ^{1}H NMR (400 MHz, $CDCl_3$) δ: 8.80 (d, J = 4.4 Hz, 1H), 7.33 (dd, J = 9.0, 4.4 Hz, 1H), 6.93 (d, J = 9.0 Hz, 1H), 4.57 (q, J = 7.1 Hz, 2H), 1.43 (t, J = 7.1 Hz, 3H). MS (ESI) $(M + H)^+$ 125.

1-[6-(Ethyloxy)pyrazolo[1,5-*b*]pyridazin-3-yl]ethanone (40c). In a similar manner to that described in the general procedure for compounds **16**−**21** and **29**−**37** (method a), we obtained the title compound from 3-(ethyloxy)pyridazine as a brown solid. ^{1}H NMR (300 MHz, $CDCl_3$) δ: 8.55 (d, J = 9.5 Hz, 1H), 8.26 (s, 1H), 6.96 (d, J = 9.5 Hz, 1H), 4.52 (q, J = 7.1 Hz, 2H), 2.58 (s, 3H), 1.50 (t, J = 7.1 Hz, 3H). MS (ESI) $(M + H)^+$ 206.

(2*E*)-3-(Dimethylamino)-1-[6-(ethyloxy)pyrazolo[1,5-*b*]-pyridazin-3-yl]-2-propen-1-one (40d). In a similar manner to that described in the general procedure for compounds **16**−**21** and **29**−**37** (method b), we obtained the title compound from **40c** as a brown solid. ^{1}H NMR (300 MHz, DMSO-d_6) δ: 8.57 (d, J = 9.5 Hz, 1H), 8.50 (s, 1H), 7.67 (d, J = 12.3 Hz, 1H), 7.08 (d, J = 9.5 Hz, 1H), 5.80 (d, J = 12.3 Hz, 1H), 4.40 (q, J = 7.0 Hz, 2H), 3.14 (br, 3H), 2.92 (br, 3H), 1.42 (t, J = 7.0 Hz, 3H). MS (ESI) $(M + H)^+$ 261.

4-[6-(Ethyloxy)pyrazolo[1,5-*b*]pyridazin-3-yl]-*N*-[3-(trifluoromethyl)phenyl]-2-pyrimidinamine (40). In a similar manner to that described in the general procedure for compounds **16**−**21** and **29**−**37** (method c), we obtained the title compound from **40d** as a brown solid. ^{1}H NMR (300 MHz, DMSO-d_6) δ: 9.96 (s, 1H), 9.03 (d, J = 9.5 Hz, 1H), 8.73 (s, 1H), 8.55 (d, J = 5.2 Hz, 1H), 8.31 (s, 1H), 7.99 (d, J = 7.8 Hz, 1H), 7.58 (t, J = 7.8 Hz, 1H), 7.44 (d, J = 5.2 Hz, 1H), 7.32 (d, J = 7.8 Hz, 1H), 7.15 (d, J = 9.5 Hz, 1H), 4.44 (q, J = 7.0 Hz, 2H), 1.44 (t, J = 7.0 Hz, 3H). Elemental analysis was performed for C, H, and N.

4-[6-(Propyloxy)pyrazolo[1,5-*b*]pyridazin-3-yl]-*N*-[3-(trifluoromethyl)phenyl]-2-pyrimidinamine(41). 3-Chloro-6-(propyloxy)pyridazine (41a). In a similar manner to that described for **40a**, by the reaction of 3, 6-dichloropyridazine with sodiumpropoxide, we obtained the title compound as a yellow solid. ^{1}H NMR (400 MHz, $CDCl_3$) δ: 7.33 (d, J = 9.1 Hz, 1H), 6.93 (d, J = 9.1 Hz, 1H), 4.42 (t, J = 6.7 Hz, 2H), 1.83 (m, 2H), 1.02 (t, J = 7.5 Hz, 3H). MS (ESI) $(M + H)^+$ 173.

3-(Propyloxy)pyridazine (41b). In a similar manner to that described in example **40b**, we obtained the title compound as a white solid. ^{1}H NMR (400 MHz, $CDCl_3$) δ: 8.80 (d, J = 4.4 Hz, 1H), 7.34 (m, 1H), 6.94 (d, J = 9.0 Hz, 1H), 4.46 (t, J = 6.7 Hz, 2H), 1.84 (m, 2H), 1.01 (t, J = 7.3 Hz, 3H). MS (ESI) $(M + H)^+$ 139.

1-[6-(Propyloxy)pyrazolo[1,5-*b*]pyridazin-3-yl]ethanone (41c). In a similar manner to that described in the general procedure for compounds **16**−**21** and **29**−**37** (method a), we obtained the title compound from **41b** as a brown solid. ^{1}H NMR(400 MHz, $CDCl_3$) δ: 8.51 (d, J = 9.5 Hz, 1H), 8.22 (s, 1H), 6.93 (d, J = 9.5 Hz, 1H), 4.37 (t, J = 6.6 Hz, 2H), 2.53 (s, 3H), 1.85 (m, 2H), 1.03 (t, J = 7.4 Hz, 3H). MS (ESI) $(M + H)^+$ 220.

(2*E*)-3-(Dimethylamino)-1-[6-(propyloxy)pyrazolo[1,5-*b*]pyridazin-3-yl]-2-propen-1-one (41d). In a similar manner to that described in the general procedure for compounds **16**−**21** and **29**−**37** (method b), we obtained the title compound from **41c** as a brown solid. ^{1}H NMR (300 MHz, DMSO-d^6) δ: 8.57 (d, J = 9.5 Hz, 1H), 8.50 (s, 1H), 7.67 (d, J = 12.4 Hz, 1H), 7.09 (d, J = 9.5 Hz, 1H), 5.60 (d, J = 12.4 Hz, 1H), 4.31 (t, J = 6.6 Hz, 2H), 3.14 (br, 3H), 2.92 (br, 3H), 1.82 (m, 2H), 1.03 (t, J = 7.3 Hz, 3H). MS (ESI) $(M + H)^+$ 275.

4-[6-(Propyloxy)pyrazolo[1,5-*b*]pyridazin-3-yl]-*N*-[3-(trifluoromethyl)phenyl]-2-pyrimidinamine (41). In a similar manner to that described in the general procedure for compounds **16**−**21** and **29**−**37** (method c), we obtained the title compound from **41d** as a brown solid. ^{1}H NMR (300 MHz, DMSO-d^6) δ: 9.96 (s, 1H), 9.03 (d, J = 9.6 Hz, 1H), 8.73 (s, 1H), 8.55 (d, J = 5.2 Hz, 1H), 8.31 (s, 1H), 8.00 (d, J = 8.0 Hz, 1H), 7.58 (dd, J = 8.0 and 7.8 Hz, 1H), 7.24 (d, J = 5.2 Hz, 1H), 7.33 (d, J = 7.8 Hz, 1H), 7.17 (d, J = 9.6 Hz, 1H), 4.35 (t, J = 6.6 Hz, 2H), 1.84 (m, 2H), 1.05 (t, J = 7.4 Hz, 3H). Elemental analysis was performed for C, H, and N.

4-(6-Methylpyrazolo[1,5-*b*]pyridazin-3-yl)-*N*-[3-(trifluoromethyl)phenyl]-2-pyrimidinamine (51). 1-(6-Methylpyrazolo[1,5-*b*]pyridazin-3-yl)ethanone (51a). In a similar manner to that described in the general procedure for compounds **16**−**21** and **29**−**37** (method a), we obtained the title compound from 3-methylpyridazine as a brown solid. ^{1}H NMR (300 MHz, DMSO-d^6) δ: 8.61 (d, J = 5.4 Hz, 1H), 8.39 (s, 1H), 7.23 (s, 1H), 7.19 (d, J = 5.4 Hz, 1H), 2.65 (s, 3H), 2.56 (s, 3H). MS (ESI) $(M + H)^+$ 176.

(2*E*)-3-(Dimethylamino)-1-(6-methylpyrazolo[1,5-*b*]pyridazin-3-yl)prop-2-en-1-one (51b). In a similar manner to that described in the general procedure for compounds **16**−**21** and **29**−**37** (method b), we obtained the title compound from **51a** as a brown solid. ^{1}H NMR (300 MHz, DMSO-d^6) δ: 8.60 (d, J = 5.3 Hz, 1H), 8.59 (s, 1H), 7,61 (d, J = 12.3 Hz, 1H), 7.30 (d, J = 5.3 Hz, 1H), 5.78 (d, J = 12.3 Hz, 1H), 3.23 (s, 3H), 2.86 (s, 3H), 2.51 (s, 3H). MS (ESI) $(M + H)^+$ 231.

4-(6-Methylpyrazolo[1,5-*b*]pyridazin-3-yl)-*N*-[3-(trifluoromethyl)phenyl]-2-pyrimidinamine (51). In a similar manner to that described in the general procedure for compounds **16**−**21** and **29**−**37** (method c), by the reaction of **51b**

with *N*-[3-(trifluoromethyl)phenyl]guanidine, we obtained the title compound as a brown solid. ^{1}H NMR (300 MHz, DMSO-d^6) δ: 9.96 (s, 1H), 9.04 (d, J = 9.1 Hz, 1H), 8.85 (s, 1H), 8.55 (d, J = 5.3 Hz, 1H), 8.31 (s, 1H), 8.01 (d, J = 8.2 Hz, 1H), 7.59 (dd, J = 8.2 and 7.8 Hz, 1H), 7.46 (d, J = 5.3 Hz, 1H), 7.44 (d, J = 9.1 Hz, 1H), 7.34 (d, J = 7.8 Hz, 1H), 2.62 (s, 3H). The composition of the compound was analyzed using methods A and B.

4-(6-Phenylpyrazolo[1,5-*b*]pyridazin-3-yl)-*N*-[3-(trifluoromethyl)phenyl]-2-pyrimidinamine (55). 3-Phenylpyridazine (55a). In a similar manner to that described for **40b**, we obtained the title compound from 3-chloro-6-phenylpyridazine as a white solid. ^{1}H NMR (300 MHz, $CDCl_3$) δ: 9.20 (dd, J = 4.9 and 1.5 Hz, 1H), 8.12 (m, 2H), 7.89 (dd, J = 8.5 and 1.5 Hz, 1H), 7.59 (m, 4H). MS (ESI) $(M + H)^+$ 157.

1-(6-Phenylpyrazolo[1,5-*b*]pyridazin-3-yl)ethanone (55b). In a similar manner to that described in the general procedure for compounds **16**−**21** and **29**−**37** (method a), we obtained the title compound from **55a** as a brown solid. ^{1}H NMR (300 MHz, DMSO-d^6) δ: 8.83 (s, 1H), 8.72 (d, J = 9.5 Hz, 1H), 8.19 (d, J = 9.5 Hz, 1H), 8.16 (m, 2H), 7.61 (m, 3H), 2.59 (s, 3H). MS (ESI) $(M + H)^+$ 238.

(2*E*)-3-(Dimethylamino)-1-(6-phenylpyrazolo[1,5-*b*]pyridazin-3-yl)-2-propen-1-one (55c). In a similar manner to that described in the general procedure for compounds **16**−**21** and **29**−**37** (method b), we obtained the title compound from **55b** as a brown solid. ^{1}H NMR (300 MHz, DMSO-d^6) δ: 8.80 (d, J = 9.3 Hz, 1H), 8.75 (s, 1H), 8.14 (m, 2H), 8.04 (d, J = 9.3 Hz, 1H), 7.71 (d, J = 12.4 Hz, 1H), 7.62 (m, 3H), 5.87 (d, J = 12.4 Hz, 1H), 3.16 (br, 3H), 2.96 (br, 3H). MS (ESI) $(M + H)^+$ 293.

4-(6-Phenylpyrazolo[1,5-*b*]pyridazin-3-yl)-*N*-[3-(trifluoromethyl)phenyl]-2-pyrimidinamine (55). In a similar manner to that described in the general procedure for compounds **16**−**21** and **29**−**37** (method c), we obtained the title compound from **55c** as a brown solid. ^{1}H NMR (300 MHz, DMSO-d^6) δ: 10.02 (s, 1H), 9.22 (d, J = 9.2 Hz, 1H), 8.98 (s, 1H), 8.58 (d, J = 5.2 Hz, 1H), 8.31 (s, 1H), 8.19 (m, 2H), 8.06 (m, 2H), 7.62 (m, 4H), 7.50 (d, J = 5.2 Hz, 1H), 7.35 (d, J = 6.7 Hz, 1H). Elemental analysis was performed for C, H, and N.

***N*-Phenyl-4-(2-phenylpyrazolo[1,5-*b*]pyridazin-3-yl)-2-pyrimidinamine (57). 1-(2-Phenylpyrazolo[1,5-*b*]pyridazin-3-ylethanone (57a).** In a similar manner to that described in the general procedure for compounds **16**−**21** and **29**−**37** (method a), we obtained the title compound from 4-phenylbut-3-yn-2-one as a brown solid. ^{1}H NMR (300 MHz, d^6-DMSO) δ: 8.74 (m, 3H), 7.71−7.55 (m, 5H), 2.21 (s, 3H).

(2*E*)-3-(dimethylamino)-1-(2-phenylpyrazolo[1,5-*b*]pyridazin-3-yl)-2-propen-1-one (57b). In a similar manner as that described in the general procedure for compounds **16**−**21** and **29**−**37** (method b), we obtained the title compound from **57a** as a brown solid. ^{1}H NMR (300 MHz, DMSO-d^6) δ: 8.59 (m, 3H), 7.74−7.50 (m, 6H), 5.10 (d, J = 12.5 Hz, 1H), 3.36 (brs, 3H), 2.52 (brs, 3H). MS (ESI) $(M + H)^+$ 293.

***N*-Phenyl-4-(2-phenylpyrazolo[1,5-*b*]pyridazin-3-yl)-2-pyrimidinamine (57).** In a similar manner to that described in the general procedure for compounds **16**−**21**, **29**−**37** (method c), we obtained the title compound from **57b** as a brown solid. ^{1}H NMR (300 MHz, DMSO-d^6) δ: 9.66 (s, 1H), 8.95 (d, J = 8.9 Hz, 1H), 8.65 (m, 1H), 8.35 (d, J = 5.2, 1H), 7.71−7.46 (m, 8H), 7.29 (t, J = 4.3 Hz, 2H), 6.99 (t, J = 7.8 Hz, 1H), 6.57 (d, J = 7.3 Hz, 1H). Elemental analysis was performed for C, H, and N.

4-[2-(4-Fluorophenyl)pyrazolo[1,5-*b*]pyridazin-3-yl]-*N*-phenyl-2-pyrimidinamine (63). 4-(4-Fluorophenyl)but-3-yn-2-on (63a). To a solution of 5 g (37.9 mmol) of 1-ethynyl-4-methoxybenzene in 100 mL of tetrahydrofuran was added 28.4 mL (45.4 mmol) of 1.6 M *n*-butyllithium at −78 °C. The reaction was warmed gradually from −78 °C to room temperature over a period of 2 h. The reaction was then cooled back to −78 °C, and 5.8 mL (45.7 mmol) of boron trifluoride etherate was added; after 5.0 min, 4.7 mL (49.8 mmol) of acetic anhydride was added. The reaction was warmed gradually from −78 °C to room temperature over a period of 2 h. To the reaction mixture 1 N sodium hydroxide was added until the solution was neutral. The mixture was extracted with ether (three times), and the combined ether extracts were washed with brine (three times) and dried over magnesium sulfate. The removal of the solvent under vacuum followed by purification by column chromatography with hexane/ethyl acetate (20:1) as the eluant gave 1.6 g of product as a colorless oil in 24% yield. ^{1}H NMR (300 MHz, DMSO-d^6) δ: 7.81−7.59 (m, 4H), 2.21 (s, 3H).

1-[2-(4-Fluorophenyl)pyrazolo[1,5-*b*]pyridazin-3-yl]-ethanone (63b). In a similar manner to that described in the general procedure for compounds **16**−**21** and **29**−**37** (method a), we obtained the title compound from 4-(4-fluorophenyl)-but-3-yn-2-one as a brown solid. ^{1}H NMR (300 MHz, DMSO-d^6) δ: 8.73 (m, 1H), 7.79−7.59 (m, 4H), 7.42−7.36 (m, 2H), 2.25 (s, 3H).

(2*E*)-3-(Dimethylamino)-1-[2-(4-fluorophenyl)pyrazolo-[1,5-*b*]pyridazin-3-yl]-2-propen-1-one (63c). In a similar manner to that described in the general procedure for compounds **16**−**21** and **29**−**37** (method b), we obtained the title compound from **63b** as a brown solid. ^{1}H NMR (300 MHz, DMSO-d^6) δ: 8.59 (m, 2H), 7.81 (m, 2H), 7.60 (m, 1H), 7.40 (m, 3H), 5.12 (d, J = 12.4 Hz, 1H), 3.06 (brs, 3H), 2.59 (brs, 3H); MS (ESI) $(M + H)^+$ 311.

4-[2-(4-Fluorophenyl)pyrazolo[1,5-*b*]pyridazin-3-yl]-*N*-phenyl-2-pyrimidinamine (63). In a similar manner to that described in the general procedure for compounds **16**−**21** and **29**−**37** (method c), by the reaction of **63c** with *N*-phenylguanidinium nitrate was obtained the title compound as a brown solid. ^{1}H NMR (300 MHz, DMSO-d^6) δ: 9.64 (s, 1H), 8.87 (m, 1H), 8.63 (s, 1H), 8.35 (s, 1H), 7.68−7.24 (m, 9H), 6.95 (s, 1H), 6.58 (s, 1H). Elemental analysis was performed for C, H, and N.

4-[2-(4-Methoxyphenyl)pyrazolo[1,5-*b*]pyridazin-3-yl]-*N*-phenylpyrimidin-2-amine (68). 4-(4-Methoxyphenyl)-but-3-yn-2-one (68a). In a similar manner to that described for **63a**, we obtained the title compound from 1-ethynyl-4-methoxybenzene as a colorless oil. ^{1}H NMR (300 MHz, $CDCl_3$) δ: 7.56 (d, J = 8.8 Hz, 2H), 6.93 (d, J = 8.8 Hz, 2H), 3.88 (s, 3H), 2.47 (s, 3H). MS (ESI) $(M + H)^+$ 175.

1-[2-(4-Methoxyphenyl)pyrazolo[1,5-*b*]pyridazin-3-yl]-ethanone (68b). In a similar manner to that described in the general procedure for compounds **16**−**21** and **29**−**37** (method a), we obtained the title compound from **68a** as a brown solid. ^{1}H NMR (300 MHz, DMSO-d^6) δ: 8.7 (m, 2H), 7.6 (d, J = 8.5 Hz, 2H), 7.58 (m, 1H), 7.1 (d, J = 8.5 Hz, 2H), 3.87 (s, 3H), 2.24 (s, 3H). MS (ESI) $(M + H)^+$ 268.

(2*E*)-3-(Dimethylamino)-1-[2-(4-methoxyphenyl)pyrazolo[1,5-*b*]pyridazin-3-yl]prop-2-en-1-one (68c). In a similar manner to that described in the general procedure for compounds **16**−**21** and **29**−**37** (method b), we obtained the title compound from **68b** as a brown solid. ^{1}H NMR (300 MHz, DMSO-d^6) δ: 8.53 (m, 2H), 7.68 (d, J = 8.2 Hz, 2H), 7.57 (d, J = 12.5 Hz, 1H), 7.38 (m, 1H), 7.08 (d, J = 8.2 Hz, 2H), 5.14 (d, J = 12.5 Hz, 1H), 3.84 (s, 3H), 3.06 (br, 3H), 2.57 (br, 3H). MS (ESI) $(M + H)^+$ 323.

4-[2-(4-Methoxyphenyl)pyrazolo[1,5-*b*]pyridazin-3-yl]-*N*-phenylpyrimidin-2-amine (68). In a similar manner to that described in the general procedure for compounds **16**−**21** and **29**−**37** (method c), by the reaction of **68c** with *N*-phenylguanidinium nitrate was obtained the title compound as a brown solid. ^{1}H NMR (400 MHz, DMSO-d^6) δ: 9.6 (s, 1H), 8.86 (d, J = 8.9 Hz, 1H), 8.57 (m, 1H), 8.30 (d, J = 5.2 Hz, 1H), 7.67 (d, J = 8.0 Hz, 2H), 7.55 (d, J = 8.6 Hz, 2H), 7.39 (m, 1H), 7.23 (dd, J = 8.0 Hz, 2H), 7.05 (d, J = 8.6 Hz, 2H), 6.92(dd, J = 7.3 Hz, 1H), 6.56 (d, J = 5.2 Hz, 1H), 3.80 (s, 3H). Elemental analysis was performed for C, H, and N.

***N*-Phenyl-4-{2-[4-(trifluoromethyl)phenyl]pyrazolo-[1,5-*b*]pyridazin-3-yl}pyrimidin-2-amine (73). 4-(4-Trifluorophenyl)but-3-yn-2-one (73a).** In a similar manner to that described for **63a**, we obtained the title compound from 1-ethynyl-4-(trifluoromethyl)benzene as a colorless oil. ^{1}H

NMR (300 MHz, $CDCl_3$) δ: 7.63 (m, 4H), 2.52 (s, 3H). CI-MS (M − 1) 211.

1-[2-(4-Trifluoromethylphenyl)pyrazolo[1,5-*b*]pyridazin-3-yl]ethanone (73b). In a similar manner to that described in the general procedure for compounds **16**−**21** and **29**−**37** (method a), by the reaction of **73a** was obtained the title compound as a brown solid. ^{1}H NMR (300 MHz, DMSO-d^6) δ: 8.75 (br, 1H), 8.73 (br, 1H), 7.93 (m, 4H), 7.64 (m, 1H), 2.31 (s, 3H). MS (ESI) $(M + H)^+$ 306.

(2*E*)-3-(Dimethylamino)-1-[2-(4-trifluoromethylphenyl)-pyrazolo[1,5-*b*]pyridazin-3-yl]prop-2-en-1-one (73c). In a similar manner to that described in the general procedure for compounds **16**−**21** and **29**−**37** (method b), by the reaction of **73b** was obtained the title compound as a brown solid. ^{1}H NMR (300 MHz, DMSO-d^6) δ: 8.61 (br, 1H), 8.52 (d, J = 8.8 Hz, 1H), 7.98 (d, J = 8.1 Hz, 2H), 7.98 (d, J = 8.1 Hz, 2H), 7.60 (d, J = 12.3 Hz, 1H), 7.56 (m, 1H), 5.10 (d, J = 12.3 Hz, 1H), 3.06 (br, 3H), 2.61 (br, 3H). MS (ESI) $(M + H)^+$ 306.

***N*-Phenyl-4-{2-[4-(trifluoromethyl)phenyl]pyrazolo-[1,5-*b*]pyridazin-3-yl}pyrimidin-2-amine (73).** In a similar manner to that described in the general procedure for compounds **16**−**21** and **29**−**37** (method c), by the reaction of **73c** with *N*-phenylguanidinium nitrate was obtained the title compound as a brown solid.^{1}H NMR (300 MHz, DMSO-d^6) δ: 9.68 (s, 1H), 8.86 (d, J = 8.8 Hz, 1H), 8.69 (m, 1H), 8.43 (d, J = 5.2 Hz, 1H), 7.91 (m, 4H), 7.63 (d, J = 7.9 Hz, 2H), 7.49 (m, 1H), 7.22 (dd, J = 7.9, 7.3 Hz, 2H), 6.94 (t, J = 7.3 Hz, 1H), 6.69 (d, J = 5.1 Hz). Elemental analysis was performed for C, H, and N.

***N*-Phenyl-4-{2-[3-(trifluoromethyl)phenyl]pyrazolo-[1,5-*b*]pyridazin-3-yl}-2-pyrimidinamine (78). 4-[3-(Trifluoromethyl)phenyl]-3-butyn-2-one (78a).** In a similar manner to that described for 63a, we obtained the title compound from 1-ethynyl-3-(trifluoromethyl)benzene as a colorless oil. ^{1}H NMR (300 MHz, DMSO-d^6) δ: 8.01−7.60 (m, 4H), 2.44 (s, 3H). GC-MS (CI) $(M + H)^+$ 213.

1-[2-(4-Fluorophenyl)pyrazolo[1,5-*b*]pyridazin-3-yl]-ethanone (78b). In a similar manner to that described in the general procedure for compounds **16**−**21** and **29**−**37** (method a), we obtained the title compound from **78a** as a brown solid. ^{1}H NMR (300 MHz, DMSO-d^6) δ: 8.76 (m, 2H), 8.08−7.62 (m, 5H), 2.32 (s, 3H).

(2*E*)-3-(Dimethylamino)-1-{2-[3-(trifluoromethyl)phenyl]pyrazolo[1,5-*b*]pyridazin-3-yl}-2-propen-1-one (78c). In a similar manner to that described in the general procedure for compounds **16**−**21** and **29**−**37** (method b), we obtained the title compound from 78b as a brown solid. ^{1}H NMR (300 MHz, DMSO-d^6) δ: 8.53 (m, 2H), 7.98 (m, 2H), 7.76 (m, 2H), 7.50 (m, 1H), 7.32 (m, 1H), 5.05 (d, 1H, J = 12.5 Hz), 2.97 (brs, 3H), 2.51 (brs, 3H). MS (ESI) $(M + H)^+$ 361.

***N*-Phenyl-4-{2-[3-(trifluoromethyl)phenyl]pyrazolo-[1,5-*b*]pyridazin-3-yl}-2-pyrimidinamine (78).** In a similar manner to that described in the general procedure for compounds **16**−**21** and **29**−**37** (method b), by the reaction of **78c** with *N*-phenylguanidinium nitrate was obtained the title compound as a brown solid. ^{1}H NMR (300 MHz, DMSO-d^6) δ: 9.68 (s, 1H), 8.88 (d, J = 8.8 Hz, 1H), 8.69 (m, 1H), 8.42 (d, J = 5.3 Hz, 1H), 8.02−7.74 (m, 6H), 7.65 (d, J = 8.0 Hz, 1H), 7.48 (m, 1H), 7.25 (m, 1H), 6.67 (d, J = 5.2 Hz, 1H). Elemental analysis was performed for C, H, and N.

4-[2-(4-Chlorophenyl)pyrazolo[1,5-*b*]pyridazin-3-yl]-*N*-phenylpyrimidin-2-amine (82). 4-(4-Chlorophenyl)but-3-yn-2-one (82a). In a similar manner to that described for **63a**, we obtained the title compound from 1-ethynyl-4-chlorobenzene as a colorless oil. ^{1}H NMR (400 Mz, DMSO-d^6) δ: 7.49 (d, J = 8.4 Hz, 1H), 7.39 (d, J = 8.4 Hz, 1H), 7.35 (d, J = 8.4 Hz, 1H), 7.27 (d, J = 8.5 Hz, 1H), 2.43 (s, 3H). GC−MS (CI) $(M^+ - 15)$ 163.

1-[2-(4-Chlorophenyl)pyrazolo[1,5-*b*]pyridazin-3-yl]-ethanone (82b). In a similar manner to that described in the general procedure for compounds **16**−**21** and **29**−**37** (method a), we obtained the title compound from **82a** as a brown solid. ^{1}H NMR (400 Mz, DMSO-d^6) δ: 8.68 (m, 2H), 7.69 (d, J = 8.4 Hz, 2H), 7.56 (m, 3H), 2.23 (s, 3H). MS (ESI) $(M + H)^+$ 272.

(2*E*)-1-[2-(4-Chlorophenyl)pyrazolo[1,5-*b*]pyridazin-3-yl]-3-(dimethylamino)prop-2-en-1-one (82c). In a similar manner to that described in the general procedure for compounds **16**−**21** and **29**−**37** (method b), we obtained the title compound from **82b** as a brown solid. ^{1}H NMR (300 MHz, DMSO-d^6) δ: 8.59 (m, 1H), 8.50 (d, J = 8.9 Hz, 1H), 7.78 (d, J = 8.4 Hz, 2H), 7.59 (m, 3H), 7.39 (m, 1H), 5.13 (d, J = 12.5 Hz, 1H), 3.07 (br, 3H), 2.62 (br, 3H). MS (ESI) $(M + H)^+$ 327.

4-[2-(4-Chlorophenyl)pyrazolo[1,5-*b*]pyridazin-3-yl]-*N*-phenylpyrimidin-2-amine (82). In a similar manner to that described in the general procedure for compounds **16**−**21** and **29**−**37** (method c), by the reaction of **82c** with *N*-phenylguanidinium nitrate was obtained the title compound as a brown solid. ^{1}H NMR (300 MHz, DMSO-d^6) δ: 9.67 (s, 1H), 8.89 (d, J = 8.9 Hz, 1H), 8.67 (d, J = 2.8 Hz, 1H), 8.40 (d, J = 5.0 Hz, 1H), 7.66 (m, 6H), 7.47 (m, 1H), 7.25 (dd, J = 7.4 Hz, 2H), 6.96 (t, J = 7.4 Hz, 1H), 6.64 (d, J = 5.0 Hz, 1H). Elemental analysis was performed for C, H, and N.

4-(6-Methyl-2-phenylpyrazolo[1,5-*b*]pyridazin-3-yl)-*N*-phenyl-2-pyrimidinamine (87). 1-(6-Methyl-2-phenylpyrazolo[1,5-*b*]pyridazin-3-yl)ethanone (87a). In a similar manner to that described in the general procedure for compounds **16**−**21** and **29**−**37** (method a), we obtained the title compound from 3-methylpyridazine and 4-phenylbut-3-yn-2-one as a brown solid. ^{1}H NMR (300 MHz, DMSO-d^6) δ: 8.60 (d, J = 9.2 Hz, 1H), 7.69 (m, 2H), 7.56−7.50 (m, 4H), 2.62 (s, 3H), 2.19 (s, 3H).

(2*E*)-3-(Dimethylamino)-1-(6-methyl-2-phenylpyrazolo-[1,5-*b*]pyridazin-3-yl)-2-propen-1-one (87b). In a similar manner to that described in the general procedure for compounds **16**−**21** and **29**−**37** (method b), we obtained the title compound from **87a** as a brown solid. ^{1}H NMR (300 MHz, DMSO-d^6) δ: 8.56 (m, 2H), 7.74−7.50 (m, 6H), 5.10 (d, J = 12.5 Hz, 1H), 3.36 (brs, 3H), 2.52 (brs, 3H); 2.57 (s, 3H). MS (ESI) $(M + Na)^+$ 329.

4-(6-Methyl-2-phenylpyrazolo[1,5-*b*]pyridazin-3-yl)-*N*-phenyl-2-pyrimidinamine (87). In a similar manner to that described in the general procedure for compounds **16**−**21** and **29**−**37** (method c), we obtained the title compound from **87b** as a brown solid. ^{1}H NMR (300 MHz, DMSO-d^6) δ: 9.60 (s, 1H), 8.81 (d, J = 9.1 Hz, 1H), 8.29 (d, J = 5.3 Hz, 1H), 7.69−7.21 (m 9H), 6.96 (m, 2H), 6.67 (d, J = 5.1 Hz, 1H), 2.59 (s, 3H). Elemental analysis was performed for C, H, and N.

4-{6-Methyl-2-[3-(trifluoromethyl)phenyl]pyrazolo[1,5-*b*]pyridazin-3-yl}-*N*-phenyl-2-pyrimidinamine (92). 1-{6-Methyl-2-[3-(trifluoromethyl)phenyl]pyrazolo-[1,5-*b*]-pyridazin-3-yl}ethanone (92a). In a similar manner to that described in the general procedure for compounds **16**−**21** and **29**−**37** (method a), we obtained the title compound from 3-methylpyridazine and 4-[3-(trifluoromethyl)phenyl]-3-butyn-2-one as a brown solid. ^{1}H NMR (300 MHz, DMSO-d^6) δ: 8.63 (d, J = 9.4 Hz, 1H), 8.06 (m, 2H), 7.93 (m, 1H), 7.81 (m, 1H), 7.56 (d, J = 9.2 Hz, 1H), 2.63 (s, 3H), 2.31 (s, 3H). MS (ESI) $(M + H)^+$ 320.

(2*E*)-3-(Dimethylamino)-1-{6-methyl-2-[3-(trifluoromethyl)phenyl]pyrazolo[1,5-*b*]pyridazin-3-yl}-2-propen-1-one (92b). In a similar manner to that described in the general procedure for compounds **16**−**21** and **29**−**37** (method b), we obtained the title compound from **92a** as a brown solid. ^{1}H NMR (300 MHz, DMSO-d^6) δ: 8.53 (m, 1H), 7.98 (m, 2H), 7.76 (m, 2H), 7.50 (m, 1H), 7.32 (m, 1H), 5.05 (d, J = 12.5 Hz, 1H), 2.97 (brs, 3H), 2.51 (brs, 3H), (2.58 s, 3H).

4-{6-Methyl-2-[3-(trifluoromethyl)phenyl]pyrazolo[1,5-*b*]pyridazin-3-yl}-*N*-phenyl-2-pyrimidinamine (92). In a similar manner to that described in the general procedure for compounds **16**−**21** and **29**−**37** (method b), by the reaction of **92b** with *N*-phenylguanidinium nitrate was obtained the title compound as a brown solid. ^{1}H NMR (300 MHz, DMSO-d^6) δ: 9.92 (s, 1H), 8.70 (d, J = 8.2 Hz, 1H), 8.42 (m, 1H), 8.34−7.19 (m, 10 H), 6.66 (d, J = 5.1 Hz, 1H), 2.61 (s, 3H). Elemental analysis was perfomed by methods A and B.

4-{6-Methyl-2-[4-(trifluoromethyl)phenyl]pyrazolo[1,5-*b*]pyridazin-3-yl}-*N*-phenylpyrimidin-2-amine (96). 1-{6-Methyl-2-[4-(trifluoromethyl)phenyl]pyrazolo[1,5-*b*]-

pyridazin-3-yl}ethanone (96a). In a similar manner to that described in the general procedure for compounds **16**−**21** and **29**−**37** (method a), we obtained the title compound from 3-methylpyridazine and 4-[4-(trifluoromethyl)phenyl]-3-butyn-2-one as a brown solid. ^{1}H NMR (300 MHz, DMSO-d^6) δ: 8.58(d, J = 9.3 Hz, 1H), 7.88 (m, 4H), 7.51(d, J = 9.3 Hz, 1H), 2.59 (s, 3H), 2.26 (s, 3H). MS (ESI) (M + H)+ 320.

(2*E*)-3-(Dimethylamino)-1-{6-methyl-2-[4-(trifluoromethyl)phenyl]pyrazolo[1,5-*b*]pyridazin-3-yl}prop-2-en-1-one (96b). In a similar manner to that described in the general procedure for compounds **16**−**21** and **29**−**37** (method b), we obtained the title compound from **96a** as a brown solid. ^{1}H NMR (300 MHz, DMSO-d^6) δ: 8.37 (d, J = 9.2 Hz, 1H), 7.93 (d, J = 8.3 Hz, 2H), 7.83 (d, J = 8.3 Hz, 2H), 7.54 (d, J = 12.5 Hz, 1H), 7.30 (d, J = 9.2 Hz, 1H), 5.05 (d, J = 12.5 Hz, 1H), 3.02 (s, 3H), 2.56 (s, 3H), 2.48 (s, 3H). MS (ESI) (M + H)$^+$ 374.

4-{6-Methyl-2-[4-(trifluoromethyl)phenyl]pyrazolo[1,5-*b*]pyridazin-3-yl}-*N*-phenylpyrimidin-2-amine (96). In a similar manner to that described in the general procedure for compounds **16**−**21** and **29**−**37** (method b), by the reaction of **96b** with *N*-phenylguanidinium nitrate was obtained the title compound as a brown solid. ^{1}H NMR (300 MHz, DMSO-d^6) δ: 9.62 (s, 1H), 8.71 (d, J = 9.2 Hz, 1H), 8.36 (d, J = 5.0 Hz, 1H), 7.85 (br, 4H), 7.59 (d, J = 7.8 Hz, 1H), 7.37 (d, J = 9.2 Hz, 1H), 7.32 (m, 1H), 7.18(dd, J = 7.8, 7.5 Hz, 2H), 6.91 (m, 1H), 6.62 (d, J = 5.0 Hz, 1H), 2.59 (s, 3H). Elemental analysis was performed for C, H, and N.

4-[2-(4-Fluorophenyl)-6-methylpyrazolo[1,5-*b*]pyridazin-3-yl]-*N*-phenyl-2-pyrimidinamine (98). 1-[2-(4-Fluorophenyl)-6-methylpyrazolo[1,5-*b*]pyridazin-3-yl]ethanone (98a). In a similar manner to that described in the general procedure for compounds **16**−**21** and **29**−**37** (method a), we obtained the title compound from 3-methylpyridazine and 4-[4-(fluoro)-phenyl]-3-butyn-2-one as a brown solid. ^{1}H NMR (300 MHz, DMSO-d^6) δ: 8.56 (d, J = 9.2 Hz, 1H), 7.72 (m, 2H), 7.50 (d, J = 9.3 Hz, 1H), 7.37 (m, 2H), 2.58 (s, 3H), 2.19 (m, 3H). MS (ESI) (M + H)$^+$ 270.

(2*E*)-3-(Dimethylamino)-1-[2-(4-fluorophenyl)-6-methylpyrazolo[1,5-*b*]pyridazin-3-yl]-2-propen-1-one (98b). In a similar manner to that described in the general procedure for compounds **16**−**21** and **29**−**37** (method b), we obtained the title compound from **98a** as a brown solid. ^{1}H NMR (300 MHz, DMSO-d^6) δ: 8.39 (d, J = 9.2 Hz, 1H), 7.75−7.51 (m, 2H), 7.33−7.25 (m, 3H), 5.06 (d, J = 12.5 Hz, 1H), 3.02 (brs, 3H), 2.54 (brs, 3H), 2.48 (s, 3H). MS (ESI) (M + H)$^+$ 325.

4-[2-(4-Fluorophenyl)-6-methylpyrazolo[1,5-*b*]pyridazin-3-yl]-*N*-phenyl-2-pyrimidinamine (98). In a similar manner to that described in the general procedure for compounds **16**−**21** and **29**−**37** (method c), by the reaction of **98b** with *N*-phenylguanidinium nitrate was obtained the title compound as a brown solid. ^{1}H NMR (300 MHz, DMSO-d^6) δ: 9.43 (s, 1H), 8.77 (d, J = 9.2 Hz, 1H), 8.32 (d, J = 5.2 Hz, 1H), 7.68 (m, 3H), 7.37 (m, 6H), 6.95 (t, J = 7.3 Hz, 1H), 6.55 (d, J = 5.3 Hz, 1H), 2.58 (s, 3H). Elemental analysis was performed for C, H, and N.

4-(2-Cyclopropylpyrazolo[1,5-*b*]pyridazin-3-yl)-*N*-phenylpyrimidin-2-amine (103). 4-Cyclopropylbut-3-yn-2-one (103a). In a similar manner to that described for **63a**, by the reaction of cyclopropyl acetylene with acetic anhydride was obtained the title compound as a colorless oil after column chromatography with hexane/ethyl acetate (9:1) to afford the title compound in 64% yield. ^{1}H NMR (300 MHz, $CDCl_3$) δ: 2.31 (s, 3H), 1.46−1.26 (m, 1H), 1.02−0.90 (m, 4H)). GC−MS (M + H)$^+$ 109.

1-(2-Cyclopropylpyrazolo[1,5-*b*]pyridazin-3-yl)ethanone (103b). In a similar manner to that described in the general procedure for compounds **16**−**21** and **29**−**37** (method a), we obtained the title compound from pyridazine and **103a** as a brown solid. ^{1}H NMR (300 MHz, DMSO-d^6) δ: 8.63 (m, 2H), 7.54 (dd, J = 8.9, 8.7 Hz, 1H), 2.95 (m, 1H), 2.68 (s, 3H), 1.14−1.04 (m, 4H). MS (ESI) (M + H)$^+$ 202.

(2*E*)-1-(2-Cyclopropylpyrazolo[1,5-*b*]pyridazin-3-yl)-3-(dimethylamino)prop-2-en-1-one (103c). In a similar manner to that described in the general procedure for compounds **16**−**21** and **29**−**37** (method b), we obtained the title compound from **103b** as a brown solid. ^{1}H NMR (300 MHz, DMSO-d^6) δ: 8.55 (m, 2H), 7.75 (d, J = 12.3 Hz, 1H)), 7.36 (dd, J = 9.0, 9.0 Hz, 1H), 5.75 (d, J = 12.4 Hz, 1H), 3.17 (brs, 3H), 2.92 (brs, 3H), 2.69 (m, 1H), 2.53 (s, 3H), 1.14−1.11 (m 4H). MS (ESI) (M + H)$^+$ 257.

4-(2-Cyclopropylpyrazolo[1,5-*b*]pyridazin-3-yl)-*N*-phenylpyrimidin-2-amine (103). In a similar manner to that described in the general procedure for compounds **16**−**21** and **29**−**37** (method c), by the reaction of **103c** with *N*-phenylguanidinium nitrate was obtained the title compound as a brown solid. ^{1}H NMR (300 MHz, DMSO-d^6) δ: 9.62 (s, 1H), 8.96 (d, J = 9.1 Hz, 1H), 8.56 (m, 2H), 7.83 (d, J = 7.7 Hz, 2H), 7.41−7.31 (m, 5H), 2.68 (m, 1H), 1.21−1.05 (m, 4H). Elemental analysis was performed for C, H, and N.

4-(2-Cyclohexylpyrazolo[1,5-*b*]pyridazin-3-yl)-*N*-phenylpyrimidin-2-amine (105). 4-Cyclohexylbut-3-yn-2-one (105a). In a similar manner to that described for **63a**, by the reaction of cyclohexyl acetylene with acetic anhydride was obtained the title compound as a colorless oil after column chromatography with hexane/ethyl acetate (9:1) to afford the title compound in 35% yield. ^{1}H NMR (300 MHz, $CDCl_3$) δ: 2.32 (s, 3H), 1.96−1.26 (m, 11H). GC−MS (M + H)$^+$ 151.

1-(2-Cyclohexylpyrazolo[1,5-*b*]pyridazin-3-yl)ethanone (105b). In a similar manner to that described in the general procedure for compounds **16**−**21** and **29**−**37** (method a), we obtained the title compound from pyridazine and **105a** as a brown solid. ^{1}H NMR (300 MHz, DMSO-d^6) δ: 8.65 (m, 2H), 7.55 (dd, J = 9.0, 9.0 Hz, 1H), 3.44 (m, 1H), 2.63 (s, 3H), 2.0−1.31 (m, 10H). MS (ESI) (M + H)$^+$ 244.

(2*E*)-1-(2-Cyclohexylpyrazolo[1,5-*b*]pyridazin-3-yl)-3-(dimethylamino)prop-2-en-1-one (105c). In a similar manner to that described in the general procedure for compounds **16**−**21** and **29**−**37** (method b), we obtained the title compound from **105b** as a brown solid. ^{1}H NMR (300 MHz, DMSO-d^6) δ: 8.51 (m, 2H), 7.73 (d, J = 12.3 Hz, 1H)), 7.36 (dd, J = 8.9, 8.9 Hz, 1H), 5.48 (d, J = 12.2 Hz, 1H), 3.42 (m, 1H), 3.16 (brs, 3H), 2.92 (brs, 3H), 2.14−1.38 (m 10H). MS (ESI) (M + H)$^+$ 299.

4-(2-Cyclohexylpyrazolo[1,5-*b*]pyridazin-3-yl)-*N*-phenylpyrimidin-2-amine (105). In a similar manner to that described in the general procedure for compounds **16**−**21** and **29**−**37** (method c), by the reaction of **105c** with *N*-phenylguanidinium nitrate was obtained the title compound as a brown solid. ^{1}H NMR (300 MHz, DMSO-d^6) δ: 9.61 (s, 1H), 8.82 (d, J = 8.7 Hz, 1H), 8.56 (m, 2H), 7.81 (d, J = 7.8 Hz, 2H), 7.39−7.30 (m, 3H), 7.09−6.98 (m, 2H), 3.52 (m, 1H), 2.30−1.28 (m, 10H). Elemental analysis was performed for C, H, and N.

4-[5-(2-Methoxyethoxy)pyrazolo[1,5-*b*]pyridazin-3-yl]-*N*−(3-methoxyphenyl)pyrimidin-2-amine (107). 4-Chloro-5-methoxypyridazin-3(2*H*)-one (107a). To methanol (500 mL) was added sodium (6.64 g, 0.302 mmol) followed by 4,5-dichloropyridazin-3(2*H*)-one (25.0 g, 151 mmol). The reaction mixture was refluxed under nitrogen for 48 h. The solvent was evaporated, and the contents were acidified with acetic acid to afford a solid that was filtered and washed with water, providing 19.5 g (80%) of a white solid. ^{1}H NMR (300 MHz, DMSO-d^6) δ: 13.3 (s, 1H), 8.17 (s, 1H), 4.04 (s, 3H). GC−MS (M + H)$^+$ 161.

5-Methoxypyridazin-3(2*H*)-one (107b). To 4-chloro-5-methoxypyridazin-3(2*H*)-one (3.0 g, 18.7 mmol) was added water (70 mL), 2 N sodium hydroxide (10 mL), and 10% Pd/C (0.3 g), and the contents was stirred under hydrogen at 30 psi for 16 h. After the removal of the excess hydrogen, the reaction was heated and filtered while it was hot. Cooling of the filtrate afforded a white solid that was filtered, providing 1.4 g (59%) of the desired compound. ^{1}H NMR (300 MHz, DMSO-d^6) δ: 8.21 (s, 1H), 8.17 (d, J = 2.7 Hz, 1H), 6.20 (d, J = 2.7 Hz, 1H), 4.06 (s, 3H). GC−MS (M + H)$^+$ 127.

3-Chloro-5-methoxypyridazine (107c). To 5-methoxypyridazin-3(2*H*)-one (1.0 g, 7.9 mmol) was added phosphorus-oxychloride (10 mL), and the contents was heated at 105 °C

for 15 min. After the removal of the excess reagent, the crude product was taken in dichloromethane and added slowly to an ice-cold solution of sodium bicarbonate. The organic layer was separated, and the aqueous layer was washed with dichloromethane (50 mL × 3). The combined organic phase was dried with magnesium sulfate and concentrated under vacuum to afford 0.63 g (55%) of the product. ^{1}H NMR (300 MHz, DMSO-d^6) δ: 9.03 (d, J = 2.5 Hz, 1H), 7.57 (d, J = 2.5 Hz, 1H), 4.17 (s, 3H). GC−MS (M + H)$^+$ 145.

4-Methoxypyridazine (107d). A mixture of 3.2 g (0.022 mmol) of 3-chloro-5-methoxypyridazine in 60 mL of methanol and 0.4 g of 10% palladium on carbon was hydrogenated under 30 psi overnight. The catalyst was filtered, and the solvent was removed under vacuum. The residue was redissolved in 100 mL of dichloromethane and was washed with sodium bicarbonate solution. The organic phase was separated and dried with magnesium sulfate. Concentration under vacuum afforded the product in quantative yield. ^{1}H NMR (300 MHz, DMSO-d^6) δ: 9.03 (dd, J = 9.0, 2.8 Hz, 1H), 7.30 (dd, J = 9.0, 2.5 Hz, 1H), 3.92 (s, 3H). GC−MS (M + H)$^+$ 95.

1-(5-Methoxypyrazolo[1,5-*b*]pyridazin-3-yl)ethanone (107e). In a similar manner to that described in the general procedure for compounds **16**−**21** and **29**−**37** (method a), we obtained the title compound from 4-methoxypyridazine and **107d** as a brown oil. ^{1}H NMR (300 MHz, DMSO-d^6) δ: 8.67 (s, 1H), 8.53 (d, J = 3.3 Hz, 1H), 7.86 (d, J = 3.3 Hz, 1H), 4.06 (s, 3H), 2.54 (s, 3H). MS (ESI) (M + H)$^+$ 192.

(2*E*)-3-(Dimethylamino)-1-(5-methoxypyrazolo[1,5-*b*]-pyridazin-3-yl)prop-2-en-1-one (107f). In a similar manner to that described in the general procedure for compounds **16**−**21** and **29**−**37** (method b), we obtained the title compound from **107c** as a brown oil. ^{1}H NMR (300 MHz, DMSO-d^6) δ: 8.56 (s, 1H), 8.36 (d, J = 3.3 Hz, 1H)), 7.95 (d, J = 3.3 Hz, 1H), 7.60 (d, J = 12.5, 1H), 5.77 (d, J = 12.5 Hz, 1H), 3.92 (s, 3H), 3.38 (brs, 3H), 3.33 (brs, 3H). MS (ESI) (M + H)$^+$ 233.

4-[5-(2-Methoxyethoxy)pyrazolo[1,5-*b*]pyridazin-3-yl]-*N*−(3-methoxyphenyl)pyrimidin-2-amine (107). In a similar manner to that described in the general procedure for compounds **16**−**21** and **29**−**37** (method c), by the reaction of **107f** with *N*-(3-methoxyphenyl)guanidinium nitrate was obtained the title compound as a brown solid. ^{1}H NMR (300 MHz, DMSO-d^6) δ: 9.51 (s, 1H), 8.80 (s, 1H)), 8.48 (m, 2H), 8.24 (s, 1H), 7.43−7.25 (m, 3H), 6.65 (m, 2H), 3.81 (m, 2H), 3.78 (s, 3H), 3.73 (m, 2H), 3.32 (s, 3H). Elemental analysis was performed using methods A and B.

Enzymology. Enzyme assays were performed in 96 well plates in an SPA format. Briefly, compounds were diluted in 100% DMSO and transferred in 100% DMSO. Serial 3-fold dilutions were made. The DMSO solutions were then diluted to 10 μL with H_2O. A 3X-peptide solution (10 μL) and a 3X-enzyme/ATP solution (10 μL) were then added to initiate the reaction. The assays contained 100 mM HEPES (pH 7.2), 10 mM $MgCl_2$, 0.1 mg/mL BSA, 0.3 mg/mL heparin, 1 mM DTT, 6.6% DMSO (with and without inhibitor), 2.5 μM [γ-^{32}P]ATP (0.2 μCi/well), 2.8 μM of the peptide biotin-aminohexyl-Ala-Ala-Ala-Lys-Arg-Arg-Glu-Ile-Leu-Ser-Arg-Arg-Pro-Ser(PO3)-Tyr-Arg-amide, and 20 nM enzyme. The reactions were allowed to proceed for 40 min at room temperature. The enzyme reactions were terminated by the addition of 20 μL of 250 mM EDTA (pH 8.0) and 2.5 mM unlabeled ATP. After the reactions were terminated, 195 μL of PBS containing 0.25 mg of *Streptavidin*-coated SPA beads (Amersham Pharmacia) was added to each well. The plates were allowed to equilibrate for 8−24 h prior to quantitation using a scintillation counter (Packard TopCount, 1 min/well).

Values for pIC_{50} were obtained using nonlinear regression analysis according to eq 1

$$y = \text{bkgnd} + \left(\frac{(B_0 - \text{bkgnd})}{\left(\frac{1 + [\text{inhibitor}]}{10^{-\text{pIC50}}}\right)}\right) \quad (1)$$

where B_0 is the enzymatic activity in the absence of inhibitor and y is the enzymatic activity in the presence of the compound. The average standard deviation of pIC_{50} values for this assay was 0.36.

Binding Assays. The binding affinities of compounds with pIC50 values of 8.0 or greater (in the enzyme assay) were determined using a fluorescence intensity-based competitive displacement assay. A large molar excess of a fluorescent ligand (GR34521A, 200 to 500 nM) with a known binding affinity (K_L = 10 nM) was equilibrated with 25 nM GSK-3β in 100 mM HEPES (pH 7.2), 10 mM $MgCl_2$, and 1 mM DTT. The ligand was then displaced by titration with a compound of unknown affinity. The fluorescence intensity of GR34521A (an ATP-competitive inhibitor of GSK-3 β) when bound to GSK-3β was 40-fold greater than that of free GR34521A. Consequently, displacement of GR34521A from E-GR34521A resulted in a fluorescence change. The fluorescence displacement data were normalized and fit using a fixed value of E_t (25 nM) and eq 2. $F(x)$ is the observed normalized fluorescence at each concentration of x, ΔF_∞ is the maximum change in fluorescence at infinite x, $[E_t]$ is the total concentration of enzyme, $K_{i\,app}$ is the apparent affinity of the compound for the enzyme, and x is the total concentration of the compound.

$$F(x) = 1 - \frac{\Delta F_\infty}{2[E_t]}\left(K_{i_{app}} + [E_t] + x\right) - \left(\left(K_{i_{app}} + [E_t] + x\right)^2 - 4[E_t]x\right)^{0.5} \quad (2)$$

The observed $K_{i\,app}$ of a compound at a known concentration of GR34521A, was related to the true K_i by eq 3

$$K_{i\,app} = K_i\left(1 + \frac{[L]}{K_L}\right) \quad (3)$$

where [L] is the concentration (nM) of GR34521A and K_L is the dissociation constant (10 nM) of the GR34521A/enzyme complex. The model implicitly assumes that the compound displaces GR34521A from the active site of the enzyme. K_L was determined independently by steady-state titration of the protein with excess ligand or by titration of the ligand with excess protein. The K_L value was also determined by two independent kinetic methods measuring the bimolecular association rate constant k_{on} (9.8×10^7 M^{-1}s^{-1}) and k_{off} (1.4 s^{-1}) by globally fitting rate and amplitude data. The solubility limit of GR34521A in binding buffer was 6 μM. The highest concentration used in the titration of the compounds was 400 nM. No assumptions were made with respect to the solubility of the compounds. The enzyme active site titration was determined using GR34521A. The average standard deviation of K_i values was 12% of the determined value.

General Methods. Fluorescence spectra were recorded with a Perkin-Elmer LS50B spectrofluorometer. The excitation wavelength was 360 nm, and the emission wavelength was 450 nm for GR34521A. Rapid reactions were monitored on an Applied Photophysics SX17MV spectrophotometer (Leatherhead, England). The entrance and exit slits were 2 mm in the fluorescence mode. All fluorescence data were corrected for filter effects empirically. The correction factors were determined by the titration of the compound with the ligand (GR34521A). The dynamic and static quenching contributions to the fluorescence quenching of GR34521A by compounds are minimal at the concentrations employed in these experiments. The appropriate equations were fit to the data by nonlinear least squares using SigmaPlot from Jandel Scientific (Corte Madera, CA). All determinations were made at 25 °C.

Cellular Assay. The L6 rat skeletal muscle myoblast cell line was used to study the effects of GSK-3 inhibition**.** Glycogen synthesis was measured as the incorporation of ^{14}C-glucose into ^{14}C-glycogen. Differentiated L6 cells were incubated with and without the test compound in a modified Krebs Henseleit medium with ^{14}C-glucose. The cells were then dissolved, and the ^{14}C-glycogen product separated from excess ^{14}C-glucose substrate by the binding of the glycogen to 3-mm chromatography filter paper; extensive washing with ethanol was followed by quantitation by scintillation counting. The com-

pounds were diluted just before use with 10 mM stock solutions in 100% DMSO. All dilutions were prepared in 100% DMSO in 96-well format. EC_{50} values were determined if compounds had >15% maximal activation (with respect to 1 μM insulin). The percent maximal activation was used to compare the maximal effect of the compound versus insulin effect.

Pharmacokinetic Studies in Mice. Female CD-1 nude mice (weight range 20−30 g) were dosed po with compound **99** as a solution in 99/1 PEG 400/Tween 80. Blood samples were collected prior to dosing and at 1-, 3-, and 6-h time points post-dosing via cardiac puncture with EDTA. LC−MS analyses were performed on extracts of whole blood.

Acknowledgment. We thank Randy Rutkowski, Robert Johnson, and Peter Kitrinos for analytical support. We also thank Kirk Stevens for the development of some of the synthetic work described in the paper and Brad Henke for his critical reading of the manuscript.

Supporting Information Available: Description of the synthesis and experimental data for the preparation of compounds **18**−**21**, **23**−**28**, **42**−**50**, **52**−**54**, **56**, **58**−**62**, **64**−**67**, **69**−**72**, **74**−**77**, **79**−**81**, **83**−**86**, **88**−**91**, **93**−**95**, **97**, **99**−**102**, **104**, and **106** and elemental analysis/HPLC traces for all compounds. This material is available free of charge via the Internet at http://pubs.acs.org.

References

(1) (a) Cohen, P.; Yellowlees, D.; Aitken, A.; Donella-Deana, A.; Hemmings, B. A.; Parker, P. J. Separation and Characterization of Glycogen Synthase Kinase 3, Glycogen Synthase Kinase 4 and Glycogen Synthase Kinase 5 from Rabbit Skeletal Muscle. *Eur. J. Biochem*. **1982**, *124*, 21. (b) Leloir, L. F.; Olavaria, S. H.; Goldenburg, S. H.; Carminatti, H. Biosynthesis of Glycogen from Uridine Diphosphate Glucose. *Arch. Biochem. Biophys*. **1959**, *81*, 508. (c) Mandarino, L.; Wright, K.; Verity, L.; Nichols, J.; Bell, J.; Kolterman, O.; Beck-Nielsen, H. Effects of Insulin Infusion on Human Skeletal Muscle Pyruvate Dehydrogenase, Phosphofructokinase, and Glycogen Synthase. Evidence of Their Role in Oxidative and Non Oxidative Glucose Metabolism. *J. Clin. Invest*. **1987**, *80*, 655. (d) Welsh, G. I.; Proud, C. G. Glycogen Synthase Kinase-3 is Rapidly Inactivated in Response to Insulin and Phosphorylates Eukaryotic Initation Factor eIF-2B. *Biochem. J*. **1993**, *294*, 625−629. (e) Frame S.; Cohen P. GSK-3 Takes Centre Stage More Than 20 Years after Its Discovery. *Biochem. J*. **2001**, *359*, 1−16.

(2) (a) Woodgett, J. R. Molecular Cloning and Expression of Glycogen Synthase Kinase-3/factor A. *EMBO J*. **1990** *9*, 2431−2438. (b) Lau, K. F.; Miller, C. J.; Anderton, B. H.; Shaw, P. C. Expression Analysis of Glycogen Synthase Kinase-3 in Human Tissues. *J. Pept. Res*. **1999**, *54*, 85−91.

(3) (a) DePaoli-Roach, A. A. Synergistic Phosphorylation and Activation of ATP−Mg-Dependent Phosphoprotein Phosphatase by FA/GSK-3 and Casein Kinase II. *J. Biol. Chem*. **1984**, *259*, 12144−12152. (b) Fiol, C. J.; Williams, J. S.; Chou, C. H.; Wang, W. H.; Roach, P. J.; Roeske, R. W.; Kowalczuk, M.; DePaoli-Roach, A. A. Phosphoserine as a Recognition Determinant for Glycogen Synthase Kinase-3: Phosphorylation of a Synthetic Peptide Based on the G-Component of Protein Phosphatase-1. *Arch. Biochem. Biophys*. **1988**, *267*, 797−802. (c) Moreno F. J.; Munõz-Montanõ J. R.; Avila J. Glycogen Synthase Kinase-3 Phosphorylation of Different Residues in the Presence of Different Factors: Analysis of Tau Protein. *Mol. Cell Biochem*. **1996**, *165*, 47−54.

(4) (a) Cohen, P.; Frame, S. The Renaissance of GSK3. *Nat. Rev. Mol. Cell Biol*. **2001**, *2*, 769−776. (b) Eldar-Finkelman, H. Glycogen Synthase Kinase 3: An Emerging Therapeutic Target. *Trends Mol. Med*. **2002**, *8*, 126−132. (c) Nikoulina, S. E.; Ciaraldi, T. P.; Mudaliar, S.; Carter, L.; Johnson, K.; Henry, R. R. Inhibition of Glycogen Synthase Kinase 3 Improves Insulin Action and Glucose Metabolism in Human Skeletal Muscle. *Diabetes* **2002**, *51*, 2190−2198. (d) Henriksen, E. J.; Kinnick, T. R.; Teachey, M. K.; O'Keefe, M. P.; Ring, D. B.; Johnson, K. W.; Harrison, S. D. Modulation of Muscle Insulin Resistance by Selective Inhibition of GSK-3 in Zucker Diabetic Fatty Rats. *Am. J. Physiol*. **2003**, *284*, E892−E900. (e) Ring. D. B.; Johnson, K. W.; Henriksen, E. J.; Nuss, J. M.; Goff, D.; Kinnick, T. R.; Ma, S. T.; Reeder, J. W.; Samuels, I.; Slabiak, T.; Wagman, A. S.; Hammond, M. W.; Harrison, S. D. Selective Glycogen Synthase Kinase 3 Inhibitors Potentiate Insulin Activation of Glucose Transport and Utilization In Vitro and In Vivo. *Diabetes* **2003**, *52*, 588−595. (f) Lochhead, P. A.; Coghlan, M.; Rice, S. Q. J.; Sutherland, C. Inhibition of GSK-3 Selectively Reduces Glucose-6-phosphatase and Phosphoenolpyruvate Carboxykinase Gene Expression. *Diabetes* **2001**, *50*, 937−946.

(5) (a) Sutherland, C.; Leighton, I. A.; Cohen, P. Inactivation of Glycogen Synthase Kinase-3 by Phosphorylation: New Kinase Connections in Insulin and Growth-Factor Signaling. *Biochem. J*. **1993**, *296*, 15−19. (b) Cross, D. A.; Alessi, D. R.; Cohen, P. Andjelkovich, M.; Hemmings, B. A. Inhibition of Glycogen Synthase Kinase-3 by Insulin Mediated by Protein Kinase B. *Nature* **1995**, *378*, 785−789. (c) Stambolic, V.; Woodgett, J. R. Mitogen Inactivation of Glycogen Synthase Kinase-3 in Intact Cells via Serine 9 Phosphorylation. *Biochem. J*. **1994**, *303*, 701−704. (d) Cross, D. A.; Alessi, D. R.; Vandenheede, J. R.; McDowell, H. E.; Hundal, H. S.; Cohen, P. *Biochem. J*. **1994**, *303*, 21−26. (e) Shaw, M.; Cohen, P.; Alessi, D. R. Further Evidence that the Inhibition of Glycogen Synthase Kinase-3 by IGF-1 is Mediated by PDK1/PKB-Induced Phosphorylation of Ser-9 and Not by Dephosphorylation of Tyr-216. *FEBS Lett*. **1997**, *416*, 307−311.

(6) (a) Fang, X.; Yu, S. X.; Lu, Y.; Bast, R. C.; Woodgett, J. R.; Mills, G. B. Phosphorylation and Inactivation of Glycogen Synthase Kinase 3 by Protein Kinase A. *Proc. Natl. Acad. Sci. U.S.A*. **2000**, *97*, 11960−11965. (b) Li, M.; Wang, X.; Meintzer, M. K.; Laessig, T.; Birnbaum, M. J.; Heidenreich, K. A. Cyclic AMP Promotes Neuronal Survival by Phosphorylation of Glycogen Synthase Kinase 3. *Mol. Cell. Biol*. **2000**, *20*, 9356−9363.

(7) (a) Saito, Y.; Vandenheede, J. R.; Cohen, P. The Mechanism by which Epidermal Growth Factor Inhibits Glycogen Synthase Kinase 3 in A431 Cells. *Biochem. J*. **1994**, *303*, 27−31. (b) Goode, N.; Hughes, K.; Woodgett, J. R.; Parker, P. J. Differential Regulation of Glycogen Synthase Kinase-3 by Protein Kinase C Isotypes. *J. Biol. Chem*. **1992**, *267*, 16878−16882. (c) Tsujio, I.; Tanaka, T.; Kudo, T.; Nishikawa, T.; Shinozaki, K.; Grundke-Iqbal, I.; Iqbal, K.; Takeda, M. Inactivation of Glycogen Synthase Kinase-3 by Protein Kinase C: Implications for Regulation of Tau Phosphorylation. *FEBS Lett*. **2000**, *469*, 111−117. (d) Domínguez, J. E.; Muñoz, M. C.; Zafra, D.; Sánchez-Pérez, I.; Baqué, S.; Caron, M.; Mercurio, C.; Barberà, A.; Perona, R.; Gomis, R.; Guinovart, J. J. The Antidiabetic Agent Sodium Tungstate Activates Glycogen Synthesis through an Insulin Recepter-Independent Pathway. *J. Biol. Chem*. **2003**, *278*, 42785−42794.

(8) (a) Hughes, K.; Nikolakaki, E.; Plyte, S. E.; Totty, N. F.; Woodgett, J. R. Modulation of the Glycogen Synthase Kinase-3 Family by Tyrosine Phosphorylation. *EMBO J*. **1993**, *12*, 803−808. (b) Wang, Q. M.; Fiol, C. J.; DePaoli-Roach, A. A.; Roach, P. J. Glycogen Synthase Kinase-3 is a Dual Specificity Kinase Differentially Regulated by Tyrosine and Serine-Threonine Phosphorylation. *J. Biol. Chem*. **1994**, *269*, 14566−14574. (c) Kim, L.; Liu, J.; Kimmel, A. R. The Novel Tyrosine Kinase ZAK1 Activates GSK3 to Direct Cell Fate Specification. *Cell* **1999**, *99*, 399−408. (d) Lesort, M.; Jope, R. S.; Johnson, G. V. W. Insulin Biphasically Modulates Tau Phosphorylation: Involvement of Glycogen Synthase Kinase-3 and Fyn Tyrosine Kinase. *J. Neurochem*. **1999**, *72*, 576−584. (e) Hartigan, J. A.; Johnson, G. V. W. Transient Increases in Intracellular Calcium Result in Prolonged Site-Selective Increases in Tau Phosphorylation through a Glycogen Synthase Kinase 3 Dependent Pathway. *J. Biol. Chem*. **1999**, *274*, 21395−21401. (f) Bhat, R. V.; Shanley, J.; Correll, M. P.; Fieles, W. E.; Keith, R. A.; Scott, C. W.; Lee, C. M. Regulation and Localization of Tyrosine216 Phosphorylation of Glycogen Synthase Kinase-3 in Cellular and Animal Models of Neuronal Degeneration. *Proc. Natl. Acad. Sci. U.S.A*. **2000**, *97*, 11074−11079.

(9) Lovestone, S.; Reynolds, C. H.; Latimer, D.; Davis, D. R.; Anderton, B. H.; Gallo, J.-M.; Hanger, D.; Mulot, S.; Marquardt, B. Alzheimer's Disease-Like Phosphorylation of the Microtubule-Associated Protein Tau by Glycogen Synthase Kinase-3 in Transfected Mammalian Cells. *Curr. Biol*. **1994**, *4*, 1077.

(10) Phiel, C. J.; Wilson, C. A.; Lee, V. M.-Y.; Klein, P. S. GSK-3α Regulates Production of Alzheimer's Disease Amyloid-β Peptides. *Nature* **2003**, *423*, 435−438.

(11) (a) Martinez, A.; Castro, A.; Dorronsoro, I.; Alonso, M. Glycogen Synthase Kinase 3 (GSK-3) Inhibitors as New Promosing Drugs for Diabetes, Neurogeneration, Cancer, and Inflammation. *Med. Res. Rev*. **2002**, *22*, 373−384. (b) Beals, C. R.; Sheridan, C. M.; Turck, C. W.; Gardner, P.; Crabtree, G. R. Nuclear Export of NFATc Enhanced by Glycogen Synthase Kinase-3. *Science*, **1997**, *275*, 1930−1933. (c) Graef, I. A.; Mermelstein, P. G.; Stankunas, K.; Neilson, J. R.; Deis-seroth, K.; Tsien, R. W.; Crabtree, G. R. L-Type Calcium Channels and GSK-3 Regulate the Activity of NFATc4 in Hippocampal Neurons. *Nature* **1999**, *401*, 703−708. (d) Haq, S.; Choukroun, G.; Kang, Z. B.; Ranu, H.; Matsui, T.; Rosen-zweig, A.; Molkentin, J. D.; Alessandrini, A.; Woodgett, J.; Haj-jar, R.; Michael, A.; Force, T. Glycogen Synthase Kinase-3 is a Negative Regulator of Cardiomyocyte Hypertrophy. *J. Cell. Biol*. **2000**, *151*, 117−130. (e) Xavier, I. J.; Mercier, P. A.; McLoughlin, C. L.; Ali, A.; Woodgett, J. R.; Ovsenek, N. Glycogen

Synthase Kinase 3 Negatively Regulates Both DNA-Binding and Transcriptional Activities of Heatshock Factor 1. *J. Biol. Chem*. **2000**, *275*, 29147−29152. (f) Hedgepeth, C. M.; Conrad, L. J.; Zhang, J.; Huang, H. C.; Lee, V. M.; Klein, P. S. Activation of the Wnt Signaling Pathway: A Molecular Mechanism for Lithium Action. *Dev. Biol*. **1997**, *185*, 82−91. (g) Rubinfeld, B.; Albert, I.; Porfiri, R.; Fiol, C.; Munemitsu, S.; Polakis, P. Binding of GSK3 to the APC-β-Catenin Complex and Regulation of Complex Assembly. *Science* **1996**, *272*, 1023−1026. (h) Sakanaka, C.; Weiss, J. B.; Williams, L. T. Bridging of β-Catenin and Glycogen Synthase-3 by Axin and Inhibition of β-Catenin Mediated Transcription. *Proc. Natl. Acad. Sci. U.S.A*. **1998**, *95*, 3020−3023. (i) Yost, C.; Farr, G. H.; Pierce, S. B.; Ferkey, D. M.; Chen, M. M.; Kimelman, D. GBP, an Inhibitor of GSK-3, Is Implicated in Xenopus Development and Oncogenesis. *Cell* **1998**, *93*, 1031−1041. (j) Hoeflich, K. P.; Luo, J.; Rubie, E. A.; Tsao, M.-S.; Jin, O.; Woodgett, J. R. Requirement for Glycogen Synthase Kinase-3 in Cell Survival and NF-κB Activation. *Nature* **2000**, *406*, 86−90. (k) Henriksson, M.; Bakardjiev, A.; Klein, G.; Luscher, B. Phosphorylation Sites Mapping the N-Terminal Domain of c-myc Modulates Its Transforming Potential. *Oncogene* **1993**, *8*, 3199−3209. (l) Pulverer, B. J.; Fisher, C.; Vousden, K.; Littlewood, T.; Evan, G.; Woodgett, J. R. Site-Specific Modulation of c-Myc Cotransformation by Residues Phosphorylated in Vivo. *Oncogene* **1994**, *9*, 59−70.

(12) (a) Spittaels, K.; Van den Haute, C.; Van Dorpe, J.; Geerts, H.; Mer-cken, M.; Bruynseels, K.; Lasrado, R.; Vandezande, K.; Laenen, I.; Boon, T.; Van Lint, J.; Vandenheede, J.; Moechars, D.; Loos, R.; Van Leuven, F. Glycogen Synthase Kinase-3 Phosphorylates Protein Tau and Rescues the Axonopathy in the Central Nervous System of Human Four-Repeat Tau Transgenic Mice. *J. Biol. Chem*. **2000**, *275*, 41340−41349. (b) Lucas, J. J.; Hernandez, F.; Gomez-Ramos, P.; Moran, M. A.; Hen, R.; Avila, J. Decreased Nuclear β-Catenin, Tau Hyperphosphorylation and Neurodegeneration in GSK-3 Conditional Transgenic Mice. *EMBO J*. **2001**, *20*, 27−39.

(13) (a) Takashima, A.; Noguchi, K.; Sato, K.; Hoshino, T.; Imahori, K. Tau Protein Kinase-I is Essential for Amyloid Beta-Protein Induced Neurotoxicity. *Proc. Natl. Acad. Sci. U.S.A*. **1993**, *90*, 7789−7793. (b) Hetman, M.; Cavanaugh, J. E.; Kimelman, D. Xia, Z. G. Role of Glycogen Synthase Kinase-3 in Neuronal Apoptosis Induced by Trophic Withdrawal. *J. Neurosci*. **2000**, *20*, 2567−2574.

(14) (a) Ryves, W. J.; Harwood: A. J.; Lithium Inhibits Glycogen Synthase Kinase-3 by Competition for Magnesium. *Biochem. Biophys. Res. Commun*. **2001**, *280*, 720−725. (b) Zhang, F.; Phiel, C. J.; Spece, L.; Gurvich, N.; Klein, P. S. Inhibitory Phosphorylation of Glycogen Synthase Kinase-3 (GSK-3) in Response to Lithium. *J. Biol. Chem*. **2003**, *278*, 33067−33077.

(15) Davies, S. P.; Reddy, H.; Caivano, M.; Cohen, P. Specificity and Mechanism of Action of Some Commonly Used Protein Kinase Inhibitors. *Biochem. J*. **2000**, *351*, 95−105.

(16) (a) Leclerc, S.; Garnier, M.; Hoessel, R.; Marko, D.; Bibb, J. A.; Snyder, G. L.; Greengard, P.; Biernat, J.; Wu, Y. Z.; Mandelkow, E. M.; Eisenbrand, G.; Meijer, L. Indirubins Inhibit Glycogen Synthase Kinase-3 Beta and CDK5/P25, Two Protein Kinases Involved in Abnormal Tau Phosphorylation in Alzheimer's Disease- A Property Common to Most Cycline-Dependent Kinase Inhibitors? *J. Biol. Chem*. **2001**, *276*, 251−260. (b) Leost, M.; Schultz, C.; Link, A.; Wu, Y. Z.; Biernat, J.; Man-delkow, E. M.; Bibb, J. A.; Snyder, G. L.; Greengard, P.; Zaharevitz, D. W.; Gussio, R.; Senderowicz, A. M.; Sausville, E. A.; Kunick, C.; Meijer, L. Paullones are Potent Inhibitors of Glycogen Synthase Kinase-3 Beta and Cyclin-Dependent Kinase 5/p25. *Eur. J. Biochem*. **2000**, *267*, 5983−5994. (c) Meijer, L.; Thunnissen, A. M. W. H.; White, A. W.; Garnier, M.; Nikolic, M.; Tsai, L. H.; Walter, J.; Cleverley, K. E.; Salinas, P. C.; Wu, Y. Z.; Biernat, J.; Mandelkow, E. M.; Kim, S. H.; Pettit, G. R. Inhibition of Cyclin-Dependent Kinases, GSK-3 Beta and CK1 by Hymenialdisine, A Marine Sponge Constituent. *Chem. Biol*. **2000**, *7*, 51−63. (d) Smith, D. G.; Buffet, M.; Fenwick, A. E.; Haigh, D.; Ife, R. J.; Saunders: M.; Slingsby, B. P.; Stacey, R.; Ward, R. W. 3-Anilino-4-arylmaleimides: Potent and Selective Inhibitors of Glycogen Synthase Kinase-3 (GSK-3). *Bioorg. Med. Chem. Lett*. **2001**, *11*, 635−639. (e) Cline, G. W.; Johnson, K.; Regittnig, W.; Perret, P.; Tozzo, E.; Xiao, L.; Damico, C.; Shulman, G. I. Effects of A Novel Glycogen Synthase Kinase-3 Inhibitor on Insulin-Stimulated Glucose Metabolism in Zucker Diabetic Fatty (fa/fa) Rats. *Diabetes* **2002**, *51*, 2903−2910. (f) Bowler, A. N.; Engelhardt, S.; Sørensen, A. R.; Ursø, B.; Böd-varsdóttir, T. B.; Worsaae, H.; Hansen, B. F.; Kutzhalz, P. *2,4-Diaminothiazoles: A Novel Class of Glycogen Synthase Kinase-3 (GSK-3) Inhibitors*. Presented at the 11th RSC-SCI Medicinal Chemistry Symposium, September 9−12, 2001, Cambridge, U.K., 2001. (g) Naerum, L.; Norskov-Lauritsen, L.; Olesen, P. H. Scaffold Hopping and Optimization towards Libraries of Glycogen Synthase Kinase-3 Inhibitors. *Bioorg. Med. Chem. Lett*. **2002**, *12*, 1525−1528. (h) Olesen, P. H.; Sørensen, A. R.; Ursø, B.; Kurtzhals, P.; Bowler, A. N.; Ehrbar, U.; Hansen, B. F. Synthesis and in Vitro Characterization of 1-(4-Aminofurazan-3-yl)-5-dialkylaminomethyl-1H-[1,2,3]triazole-4-carboxylic Acid Derivatives. A New Class of Selective GSK-3 Inhibitors. *J. Med. Chem*. **2003**, *46*, 3333−3341. (i) Witherington, J.; Bordas, V.; Garland, S. L.; Hickey, D. M. B.; Ife, R. J.; Liddle, J.; Saunders: M.; Smith, D. G.; Ward, R. W. 5-Aryl-pyrazolo [3,4-b]pyridines: Potent Inhibitors of Glycogen Synthase Kinase-3 (GSK-3). *Bioorg. Med. Chem. Lett*. **2003**, *13*, 1577−1580. (j) Bax, B.; Carter, P. S.; Lewis, C.; Guy, A. R.; Bridges, A.; Tanner, R.; Pettman, G.; Mannix, C.; Culbert, A. A.; Brown, M. J. B.; Smith, D. G.; Reith, A. D. The Structure of Phosphorylated GSK-3β Complexed with a Peptide, FRATtide, That Inhibits β-Catenin Phosphorylation. *Structure* **2001**, *9*, 1143−1152. (k) Witherington, J.; Bordas, V.; Haigh, D.; Hickey, D. M. B.; Ife, R. J.; Rawlings, A. D.; Slingsby, B. P.; Smith, D. G.; Ward, R. W. 5-Aryl-pyrazolo [3,4-b]pyridazines: Potent Inhibitors of Glycogen Synthase Kinase-3 (GSK-3). *Bioorg. Med. Chem. Lett*. **2003**, *13*, 1581−1584. (l) Olesen, P. H.; Sorensen, A. R.; Urso, B.; Kurtzhals, P.; Bowler, A. N.; Ehrbar, U.; Hansen, B. F. Synthesis and in Vitro Characterization of 1-(4-Aminofurazan-3-yl)-5-dialkylaminomethyl-1-H-[1,2,3]-triazole-4-carboxylic Acid Derivatives. A new Class of Selective GSK-3 Inhibitors. *J. Med. Chem*. **2003**, *46*, 3333−3341. (m) Kuo, G.-H,; Prouty, C.; DeAngelis, A.; Shen, L.; O'Neill, D. J.; Shah, C.; Connolly, P. J.; Murray, W. V.; Conway, B. R.; Cheung, P.; Westover, L.; Xu, J. Z.; Look, R. A.; Demarest, K. T.; Emanuel, S.; Middleton, S. A.; Jolliffe, L.; Beavers, M. P.; Chen, X. Synthesis and Discovery of Macrocyclic Polyoxygenated Bis-7-azaindolyimaleimides As A Novel Series of Potent and Highly Selective Glycogen Synthase Kinase-3β Inhibitors. *J. Med. Chem*. **2003**, *46*, 4021−4031. (n) Bramson, N. H.; Corona, J.; Davis, S. T.; Dickerson, S. H.; Edelstein, M.; Frye, S. V.; Gampe, R. T.; Harris, P. A. Jr.; Hassell, A.; Holmes, W. D.; Hunter, R. N.; Lackey, K. E.; Lovejoy, B.; Luzzio, M. J.; Montana, V.; Rocque, W. J.; Rusnak, D.; Shewchuk, L.; Veal, J. M.; Walker, D. H.; Kuyper, L. F. Oxindole-Based Inhibitors of Cyclin-Dependent Kinase 2 (CDK2): Design, Synthesis, Enzymatic Activities, and X-ray Crystallographic Analysis. *J. Med. Chem*. **2001**, *44*, 4339−4358.

(17) (a) Martinez, A.; Alonso, M.; Castro, A.; Perez, C.; Moreno, F. J. First Non-ATP Competitive Glycogen Synthase Kinase 3 Beta (GSK-3 Beta) Inhibitors: Thiadiazolidinones (TDZD) as Potential Drugs for the Treatment of Alzheimer's Disease. *J. Med. Chem*. **2002**, *45*, 1292−1299. (b) Conde, S.; Perez, D. I.; Martinez, A.; Perez, C.; Moreno, F. J. Thienyl and Phenyl a-Halomethyl Ketones: New Inhibitors of Glycogen Synthase Kinase (GSK-3b) from a Library of Compound Searching. *J. Med. Chem*. **2003**, *46*, 4631−4633.

(18) (a) Leost, M.; Schultz, C.; Link, A.; Yong-Zhong, W.; Biernat, J.; Mandelkow, E.-M.; Bibb, J. A.; Snyder, G. L.; Greengard, P.; Zaharevitz, D. W.; Gussio, R.; Senderowicz, A. M.; Sausville, E. A.; Kunick, C.; Meijer, L. Paullones Are Potent Inhibitors of Glycogen Synthase Kinase-3β and Cyclin-Dependent Kinase 5/p25 *Eur. J. Biochem*. **2000**, *267*, 5983 and references therein. (b) Mettey, Y.; Gompel, M.; Thomas, V.; Garnier, M.; Leost, M.; Ceballos-Picot, I.; Noble, M.; Endicott, J.; Vierfond, J.-M.; Meijer, L. Aloisines, A New Family of CDK/GSK-3 Inhibitors. SAR, Crystal Structure in Complex with CDK2, Enzyme Selectivity, and Cellular Effects. *J. Med. Chem*. **2003**, *46*, 222−236. (c) Polychronopoulos, P.; Magiatis, P.; Skaltsounis, A.-L.; Myrianthopoulos, V.; Mikros, E.; Tarricone, A.; Musacchio, A.; Roe, M. S.; Pearl, L.; Leost, M.; Greengard, P.; Meijer, L. Structural Basis for the Synthesis of Indirubins as Potent and Selective Inhibitors of Glycogen Synthase Kinase-3 and Cyclin-Dependent Kinases. *J. Med. Chem*. **2004**, *47*, 935−946.

(19) (a) Morgan, D. O. Cyclin-Dependent Kinases: Engines, Clocks, and Microprocessors. *Annu. Rev. Cell Dev. Biol*. **1997**, *13*, 261−291. (b) Stein, G.; Baserga, R.; Giordano, A.; Denhardt, D. T. *The Molecular Basis of Cell Cycle and Growth Control*; John Wiley & Sons: New York, 1998; p 389. (c) Berthet, C.; Aleem, E.; Coppola, V.; Tessarollo, L.; Kaldis, P. Cdk2 Knockout Mice Are Viable. *Curr. Biol*. **2003**, *13*, 1775−1785.

(20) Kasuga K.; Hirobe, M.; Okamoto, T. Reaction of *N*-aminopyridinium Derivatives. XIII. Syntheses of Pyrazolodiazines by Cyclization of *N*-aminodiazinium Salts. *Chem. Pharm. Bull*. **1974**, *22*, 1814−1826.

(21) Rolf, P.; William, H. A.; John, H. W.; Marvin, R. F.; Bernard, J. D.; Robert, L. H.; John, D. P.; Suresh, K. S.; Yang, L. I. Preparation of Substituted *N*-phenyl-4-aryl-2-pyrimidinamines as Mediator Release Inhibitors. *J. Med. Chem*. **1993**, *36*, 2716−2725

(22) Sonogashira, K. Development of Pd−Cu Catalyzed Cross-Coupling of Terminal Acetylenes with sp2-Carbon Halides. *J. Organomet. Chem*. **2002**, *653*, 46−49.

JM040063I